DOKUZ EYLÜL UNIVERSITY
GRADUATE SCHOOL OF NATURAL AND APPLIED SCIENCES

EFFECTS OF AGGREGATE MINERALOGY AND CRUSHER TYPE ON THE SURFACE PROPERTIES OF HOT MIX ASPHALT

by
Amir ONSORI

July, 2012
IZMIR

EFFECTS OF AGGREGATE MINERALOGY AND CRUSHER TYPE ON THE SURFACE PROPERTIES OF HOT MIX ASPHALT

A Thesis Submitted to the
Graduate School of Natural and Applied Sciences of Dokuz Eylül University
In Partial Fulfillment of the Requirements for the Degree of Master of Science
in Civil Engineering, Transportation Program

by

Amir ONSORI

July, 2012
IZMIR

M.Sc THESIS EXAMINATION RESULT FORM

We have read the thesis entitled "**EFFECTS OF AGGREGATE MINERALOGY AND CRUSHER TYPE ON THE SURFACE PROPERTIES OF HOT MIX ASPHALT**" completed by **Amir ONSORI** under supervision of **Assoc. Prof. Dr. Burak ŞENGÖZ** and we certify that in our opinion it is fully adequate, in scope and in quality, as a thesis for the degree of Master of Science.

Assoc. Prof. Dr. Burak ŞENGÖZ

Supervisor

Assoc. Prof. Dr. Ali TOPAL

(Jury Member)

Assoc. Prof. Dr. Gökdeniz NEŞER

(Jury Member)

Prof. Dr. Mustafa SABUNCU

Director

Graduate School of Natural and Applied Sciences

ACKNOWLEDGEMENTS

It would not have been possible to write this master thesis without the help and support of the kind people around me, to only some of whom it is possible to give particular mention here.

First and foremost I want to thank my advisor, Assoc. Prof. Dr. Burak Sengoz, for his continuing help, valuable guidance and constructive criticism that led to the completion of the study. His everlasting energy, wide knowledge and active mentorship made my research at the Dokuz Eylul University very memorable. His positive attitude inspired me greatly as well. Herein, I would also give my sincere thanks to Assoc. Prof. Dr. Ali Topal. Dr. Topal's great personality, strong background in Transportation engineering and his continuing help contributed to the completion of this thesis. Thanks are also given to Assoc. Prof. Dr. Serhan Tanyel for his support throughout my master study.

I am thankful to Dr. Cagri Gorkem for his valuable helps and supports during the development of this thesis. During my study at Dokuz Eylul University, I had the opportunity to work and interact with many enthusiastic and hard working people of the department of Transportation Engineering. I would like to thank the members of the department: Eng. Kiarash Ghasemlou, Eng. Julide Oglumluoglu, Eng. Metin Mutlu Aydin, Eng. Peyman Aghazadeh, Dr. Mustafa Ozuysal and Dr. Pelin Caliskanelli for their help in processing of the thesis.

Last but not the least; I would like to thank my family for all their love and encouragement. For my parents who raised me with a love of science and supported me in all my pursuits. Thank you all.

Amir Onsori

EFFECTS OF AGGREGATE MINERALOGY AND CRUSHER TYPE ON THE SURFACE PROPERTIES OF HOT MIX ASPHALT

ABSTRACT

One of the most important properties of flexible pavements in terms of tire-pavement interface is surface texture. The texture of the pavement surface and it is ability to resist the polishing effect of traffic is of prime importance in providing skidding resistance. Pavement surface macrotexture greatly contributes to tire-pavement skid resistance which has a direct effect on traffic operation and safety particularly at high speeds. Doubtless, there exists a close relationship between the surface texture and the angularity characteristics of the aggregates within the pavement system.

The study describes the evaluation of the angularity characteristics of the aggregates crushed with different types of crushers, and their impact on the surface properties of the pavements such as texture and surface friction. For this purpose, Limestone and Basalt aggregates were prepared using impact, jaw, and roll crushers. Following the determination of the angularity characteristics of the aggregate using ASTM C1252 and modified ASTM C1252, involving two different test methods (Methods A and B), and the EN 933-6. The asphalt slabs (65x65 cm) have been prepared and compacted at their optimum bitumen contents. Surface properties of the slabs have been studied using sand patch method and laser scanner. The frictional properties have been also determined by means of Dynamic Friction Tester (DFT). Finally, evaluations have been made to determine the relationship of aggregate angularity and the surface properties.

Keywords: Aggregate angularity, aggregate mineralogy, crushers, pavement surface friction, pavement surface texture, MTD, MPD, DFT

AGREGA MİNEOROLOJİSİ İLE KIRICI TİPİNİN BİTÜMLÜ SICAK KARIŞIM YÜZEY DOKUSU ÜZERİNE ETKİLERİNİN DEĞERLENDİRİLMESİ

ÖZ

Esnek kaplamalarda en önemli parametrelerden biri yüzey doku özelliğidir. Kayma direncinin iyileştirilmesinde kaplama yüzeyinin dokusu ve trafik etkisinden kaynaklanan cilalanmaya karşı direnç yeteneği önemli bir yer teşkil etmektedir. Kaplamalarda sürtünme etkisi, kaplamanın yüzeyi ile tekerlek arasında meydana gelmektedir. Kaplama yüzeyindeki makro doku yüksek hızlardaki duruş mesafesi ile birebir ilişkilidir. Bu ilişki, kaplama içerisinde yer alan agregaların köşelilik karakteristiklerine bağlıdır.

Bu çalışma, farklı kırıcı tipleri ile elde edilen agregaların köşelilik özelliklerinin değerlendirilmesi ve kaplamalardaki doku ve sürtünme üzerine etkisinin değerlendirilmesinin kapsamaktadır. Bu amaçla, kalker ve bazalt agregaları darbeli, çeneli ve merdaneli kırıcılarla istenilen boyutlarda hazırlanmıştır. Agregalara ait köşelilik karakteristiklerinin belirlenmesi için ASTM C1252 (yöntem A ve B) ve EN 933-6 şartnameleri kullanılmıştır. Deney numuneleri 65x65 cm boyutlarında hazırlanmış olup, belirlenen optimum bitüm içerikleri ile karıştırılarak sıkıştırılmıştır. Numuneler üzerinde yüzey özelliklerinin belirlenmesi amacı ile kum yama deneyi ve lazer görüntüleme işlemleri uygulanmıştır. Bunlara ek olarak, sürtünme özellikleri dinamik sürtünme cihazı (DFT) cihazını kullanılarak belirlenmiştir. Elde edilen sonuçlar agrega köşeliliği ve yüzey özellikleri arasındaki ilişkinin tespitinde kullanılmıştır.

Anahtar sözcükler: Agrega köşeliliği, agrega mineralojisi, agrega kırıcıları, kaplama yüzey sürtünmesi, kaplama yüzey dokusu, MTD, MPD, DFT

CONTENTS

Page

CHAPTER ONE
INTRODUCTION

1.1 Introduction

Each year an unacceptably large number of fatalities and injuries resulting from accidents on highways make roadway safety one of the most important international issues. With continuous growth in the amount of highway traffic and capacity, traffic crashes increase annually over the whole world. Along this increase, a great demand and focus on the needs for safer roads and highways become prior in road projects.

While economic design of highway facilities may seem prior in road projects, nowadays the terms “safe” and “safety” are prominently included in projects and it’s generally said that safety is as prior as economy, as in long service periods, safer roads are simultaneously more economic. In addition to security factors such as highway geometry, operating speed driver dynamics and pavement surface properties also critical factors in highway safety. A proper design to provide adequate pavement surface properties and practically monitoring pavement surface properties of a project have been a high priority in recent projects worldwide.

Many factors influence the pavement surface properties such as (Chelliah et al., 2003):

- Road surface properties including texture and friction,
- Age of the road surface,
- Seasonal variation,
- Traffic intensity,
- Aggregate properties,
- Road geometry.

Among these categories, road surface properties as well as aggregate mineralogical properties gained attention in the last decade. Therefore, it is crucial to investigate and understand the factors contributing to roadway accidents. Specifically, investigation of a potential relationship between quantifiable pavement surface characteristics, such as friction and texture, and aggregate characteristics will help better understand and mitigate the problem.

The available friction on pavement surfaces depends on surface microtexture and macrotexture. Improved and durable friction can be achieved through increased textures. Microtexture, which is primarily a function of aggregate surface characteristics, is needed to provide a rough surface that disrupts the continuity of the water film and produces frictional resistance between the tire and pavement by creating intermolecular bonds. Macrotexture, which primarily depends on aggregate gradation and method of construction, provides surface drainage paths for water to drain faster from the contact area between the tire and pavement. Macrotexture helps to prevent hydroplaning and improve wet frictional resistance particularly at high speed (Fulop et al., 2000; Hanson and Prowell, 2004; Kowalski, 2007).

The surface properties of hot mix asphalt (HMA) are also affected substantially by the characteristics of aggregates, admitting shape, angularity and surface texture. The hypothesis behind this research is that it is possible to improve the frictional performance of the pavement surface by the selection of aggregate angularity characteristics and mineralogical types of aggregates.

This research aims to characterize the surface properties of Hot Mix Asphalt slabs by way of texture and friction measurements. Two types of aggregate (Basalt, Limestone and their mixture) were crushed with three different types of crushers (Impact crusher, Jaw crusher and Roll crusher) and mixed with 50/70 penetration grade bitumen to build a dense graded mixture.

Surface texture measurements included sand patch method as well as 3D laser scanner. Friction characteristics are determined by Dynamic Friction Tester.

CHAPTER TWO
AGGREGATES FOR BITUMINOUS MIXTURES

2.1 Sources of Aggregates

"Aggregate" is a collective term for the mineral materials such as sand, gravel and crushed stone that are used with a binding medium (such as water, bitumen, Portland cement, lime, etc.) to form compound materials (such as asphalt concrete and portland cement concrete). By volume, aggregate broadly accounts for 92 to 96 percent of hot mix asphalt HMA and about 70 to 80 percent of Portland cement concrete (PCC). Aggregate is also used for base and subbase courses for both flexible and rigid pavements.

Aggregates can either be natural or manufactured. Natural aggregates are mostly extracted from larger rock formations through an open excavation (Figure 2.1). Extracted rock is commonly reduced to useable sizes by mechanically skillful crushing. Factory-made aggregate is often the by-product of other manufacturing industries. The majority of aggregates applied in road construction are obtained from naturally occurring deposits, natural aggregates such as sand and gravel obtained from transported deposits, river deposits, alluvial fans and glacial outwash. Processed aggregates are obtained by crushing and screening of quarried rock, oversize gravel and boulders. Crushing brings down the size of the rock particles to make them appropriate for consumption in bituminous mixtures. Crushing also changes the texture and shape of the particles. Screening follows crushing that is used to align the particle size and particularly to eliminate the very fine or the very large particles (Topal & Sengoz, 2005).

Synthetic aggregates may be obtained as a by-product of some industrial actions or from the processing of raw materials for last use as aggregates.

Figure 2.1 Aggregate quarry

2.2 Classification of Aggregate

Mineral aggregates may be classified into two broad categories: petrological classification and mineralogical classification:

2.2.1 Petrological Classification

Rocks are classified into three major groups based on their origin of formation: Igneous, sedimentary, and metamorphic rocks.

2.2.1.1 Igneous Rocks:

"Rocks that have solidified from a fluid silicate melt or magma taking place either beneath or at the earth's surface. Their fabrics depend on their crystallization environment. If cooling progresses very slowly beneath the surface, crystallization occurs slowly and the resulting crystals are coarse grained. These rock formations are termed intrusive and plutonic. Rocks formed in this environment are granite, syenite, diorite and gabbro. If cooling takes place rapidly at or near the earth's surface the resulting crystals are small, the rock is microcrystalline. If the cooling is very rapid, the rock is cryptocrystalline or even glassy. These fine-grained rocks are basalt, andesite and rhyolite. Between the intrusive and extrusive igneous rocks, the minor intrustive (hypabyssal) rocks are found. These are dolerite, porphyrite and quartz

porphyry. The hypabyssal rocks are found generally in dykes and sills" (Wills, 1984; Topal, 2001).

2.2.1.2 Sedimentary Rocks

Rocks that have been formed by consolidation at atmospheric conditions, or cementing of deposited fragmentary materials that have been eroded from preexisting rocks, or by the concentration of inorganic materials by chemical and/or mechanical progress. Sedimentary rocks are divided in to two main groups according to their formation modes: clastic rocks and sedimentary rocks formed in-situ.

Clastic rocks include the consolidated fragmentary materials that have been eroded from pre-existing rocks. These rocks are classified in decreasing order of grain size as conglomerate, breccia, sandstone (gritstone), and shale (mudstone).

"Limestone and flint are sedimentary rocks formed in-situ and they are used for road construction. The origins of limestones are chemical organic or the 15 combination of them. They are composed of calcium carbonate in the form of calcite, organic remains, fossils, and may also contain magnesium carbonate as magnesian limestone. Dolomitic limestone contains both the dolomite and calcite.

The most important characteristic of sedimentary or layered rocks are their flat and layered structure, bedding and stratification properties. The physical properties of sedimentary rocks depend upon the mineral composition, texture, fabric, structure, cementation, and porosity.

Most minerals in clastic sediments are the same as primary igneous rocks, sedimentary rocks and metamorphic rocks. Clastic sedimentary textures consist of the following components: sorting, roundness, packing, and fabric. Sorting indicates the degree of similarity of grain sizes that reflect the transporting agent. Roundness of grains exhibits the degree of abrasion by the sharpness of the edges and corners.

Packing of grains shows the relationship of the grains or to inter granular spacing. Fabric of sediments expresses the grain orientation" (Collis & Fox, 1985).

2.2.1.3 Metamorphic Rocks

Rocks formed by the mineralogical, chemical and structural alteration of preexisting igneous and sedimentary rocks caused by the effect of temperature and pressure. Main rocks of this group are slate, crystalline marble, quartzite, greenstone and serpentine (Collis & Fox, 1985).

"*These rocks are classified into two main groups. Contact metamorphic rocks, which alteration has been caused by the action intense heat at cooling process and regional metamorphic rocks, which alteration has been caused by the combined action of pressure and heat in the deeps of earth's crust. Minerals of metamorphic rocks are more stable than the parent rock material. The contact metamorphic rocks are generally termed "hornfels" expects quartzite and marble. 'The action of heat' transforms the softer minerals of the country rocks in to harder (hornblende and feldspar). Hornfels are usually tough and hard, but they are rarely used for road stone. The principal regionally metamorphic rocks are schist and gneiss. Both rocks types have a banded texture*" (Collis & Fox, 1985; Topal, 2001).

2.2.2 Mineralogical Classification

Aggregate mineralogy influences the performance of bituminous mixtures. For instance, the adhesion of bitumen to the aggregate surface is higher in carbonate aggregates than in siliceous aggregates. The presence of certain minerals as coating on the surface of the aggregate particles impacts the bond with the bitumen and the propensity to absorb moisture.

"*Clay, gypsum, iron oxides, silt and minerals may have either poor adhesion with the asphalt binder or a propensity to absorb moisture and break the band between the aggregate and the asphalt. Certain minerals such as quartz and feldspars are hard and resistant to polish, enabling the asphalt mixture to maintain its skid*

resistance under the abrasive effect of traffic. Aggregates from sedimentary rocks such as limestone and dolomite, in contrast, can have a tendency to be polished under the action of traffic" (Chen, 1995).

ASTM standard C 294-86 gives a description of some of the ordinary or important minerals found in aggregates mineralogical variety helps in recognizing the properties of aggregate but cannot provide a basis for anticipating its performance in mixtures (Annual Book of ASTM Standards, 1994).

The ASTM classification of minerals is summarized below:

- Silica minerals (quartz, opal, chalcedony, tridymite, cristobalite)
- Ferromagnesian minerals
- Micaceous minerals
- Clay minerals
- Zeolites
- Carbonate minerals
- Sulfate minerals
- Iron sulfide minerals
- Iron oxides.

2.3 Physical Properties of Aggregates

The suitability of aggregates to be used in bituminous mixtures depends on their physical and mineralogical properties and also relatively at lower level on their chemical composition. The physical properties of aggregates are, gradation, particle shape, surface texture, durability, cleanliness, toughness, and absorption. These properties are primarily control the performance of mixtures.

2.3.1 Gradation (Size Distribution)

One of the important classifications of aggregates for use in bituminous mixtures is based on size distribution, which affects the stability and workability properties of mixture. The size of aggregate used in bituminous mixtures ranges from mineral filler (at least 65% by weight passing No. 200 sieve) to 25.4 mm (1 in.).

Aggregate particle size are typically divided into coarse [the particle size greater than No.4 (4.75mm) sieve, fine [Particle size between No.4 (4.75 mm) and No.200 (0.075 mm) sieve], and mineral filler [at least %70 by weight passing No.200 (0.075 mm) sieve].

The maximum particle size affects the workability and density of the mixture, and also economy. Large particle sizes reduce the consumption of pavement per unit volume of mix. However, using larger particle size makes it more difficult to obtain proper compaction in the mix, “Especially, if the maximum particle size exceeds one-half the thickness of the compacted pavement layer” (U.S. Army Corps of Engineers, 1991).

“The particle size distribution is most commonly expressed as the weight percents of particle sizes mechanically screened with sieves of square openings. Other techniques are also used to separate the particles. The most common way to define the particle size distribution though is in term of the aggregate gradation, 21 *which is expressed in terms of weight percentages of particles retained (or passing) through a set of sieves with successively decreasing opening”* (ASTM C136, 1993).

The gradation curve is the graphical representation of the particle size distribution with the ordinate defining the percent by weight passing a given size on an arithmetic scale, while the abscissa is the sieve size plotted to a logarithmic scale.

Aggregates may be divided on the basic of gradation as follows (refer to Figure 2.1):

a) Dense-graded (Well graded)

b) Open-graded

c) One-sized (uniform gradation)

d) Gap-graded

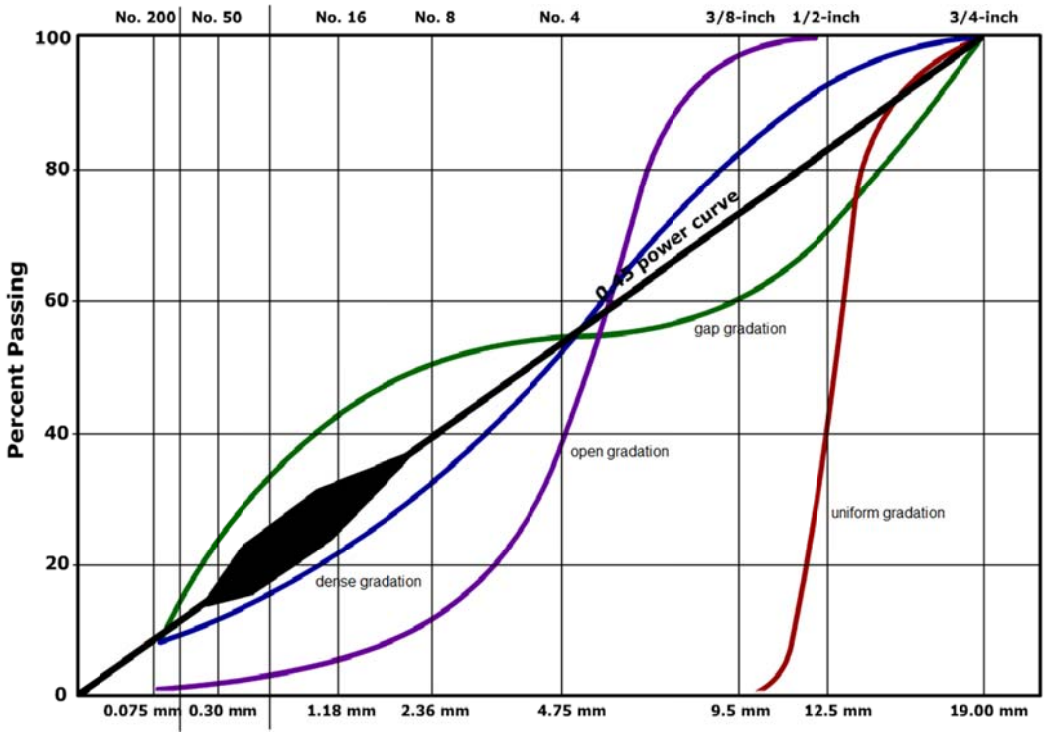

Figure 2.2 Aggregate gradation graphics (retried from http: // training.ce .washington. edu/ PGI/).

2.3.1.1 Dense-Graded Materials

"The dense-graded materials include appropriate amounts of all sizes from coarse to fine, including dust or material passing No.200. They are used in hot mix asphalts and other dense-graded types if mixtures" (Uluçaylı, 2001).

Dense-graded mixture consists of well graded aggregates and asphalt cement as binder. A dense-graded mixture with nominal size of aggregate greater than 25.4mm

(1 in.) is called a large-stone mix. By contrast, a sand mix is a dense-graded mix without course aggregates with %100 of the aggregate particles passing the 9.5 mm (3/8 in) sieve.

2.3.1.2 Open-Graded Materials

Refers to a gradation that contains only a small percentage of aggregate particles in the small range. This results in more air voids because there are not enough small particles to fill in the voids between the larger particles. The curve is near vertical in the mid-size range, and flat and near-zero in the small-size range.

Open-graded mixtures exhibit a very open structure with high permeability that allows water to drain through. Also open-graded mixtures exhibit a rough surface texture that enhances contact with vehicle tires, increasing the skid resistance.

2.3.1.3 One-Sized Materials

Refers to a gradation that contains most of the particles in a very narrow size range. In essence, all the particles are the same size. The curve is steep and only occupies the narrow size range specified.

2.3.1.4 Gap Graded Materials

Refers to a gradation that contains only a small percentage of aggregate particles in the mid-size range. The curve is flat in the mid-size range. Some PCC mix designs use gap graded aggregate to provide a more economical mix since less sand can be used for a given workability. HMA gap graded mixes can be prone to segregation during placement.

"In recent years; laboratory research and field experience have shown that gapgraded aggregates when the mixture is designed lay Gyratory Shear-Press have better resistance to rutting. In addition they give "rough" surfaces with a high coefficient of friction. They are widely used in Europe and USA" (Uluçaylı, 2001).

"Stability of a bituminous mixture depends upon the number of points of contact between individual aggregate pieces resulting in high functional resistance. The number of points of contact is higher in dense graded mixes than open-graded or one-sized mixes. The increased number of contact is points result in a greater area for load transfer from one aggregate to another. This decreases the possibility of crushing of the individual aggregate piece by points loading. Logically, it might seem that the best method of obtaining high stability in a bituminous mixture could be to use the densest gradation possible with just enough bituminous material present to bind the aggregate together. The disadvantage of this concept is that such a mix will not contain enough space for bitumen, which is necessary to assure the durability of the mixture. Durability requires a certain amount of bitumen" (Uluçaylı, 2001; Topal, 2001).

2.3.2 Particle Shape

Shape is related to three different characteristics: sphericity, form, and specially angularity (Galloway, 1994). Sphericity is a calculation of how nearly equal are the three principal axes or dimensions of a particle.

Form is the measure of the relation between the three dimensions of a particle based on ratios between the proportions of the long, medium, and short axes of the particle. Form, also called "shape factor," is used to differentiate between particles that have the same numerical sphericity (Hudson, 1999). However, different definitions exist that do not necessarily correlate. Regarding sphericity and form, particles can be classified qualitatively as cubical, spherical, or flat and elongated.

According to Kwan (2001), there are two other characteristics: roundness and angularity. Angularity is related to the sharpness of the edges and corners of a particle, while roundness attempts to describe the outline of the particle, which may be measured in terms of "convexity." Angularity can be defined numerically as the ratio of the average radius of curvature of the corners and edges of the particle to the radius of the maximum inscribed circle (Popovics, 1992).

- Angular: Little evidence of wear on the particle surface
- Subangular: Evidence of some wear, but faces untouched
- Subrounded: Considerable wear, faces reduced in area
- Rounded: Faces almost gone
- Well rounded: No original faces left

The detailed explanation of angularity and its relation with HMA performance will be held in chapter 3.

Figure 2.3 provides two comparable charts for the visual assessment of particle shape.

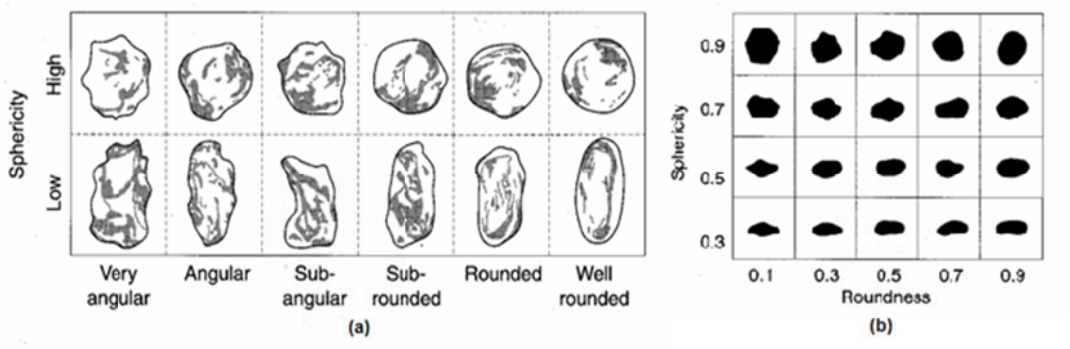

Figure 2.3 Visual assessment of particle shape (Powers, 1953; Krumbein, 1963) (a) Derived from measurements of sphericity and roundness (b) Based upon morphological observations

These shape and form definitions can be used with data acquired by measuring manually the three principal dimensions of a number of particles to characterize aggregates. Masad (2002), uses a black and white video camera and a video microscope to capture images at different resolutions and different lighting schemes.

Particle shape classification are presented in Table 2.1.

Table 2.1 Particle Shape Classification (British Standards 812, 1975,).

Classification	Description	Examples
Rounded	Fully water-wont completely shaped by attrition	River or seashore gravel ; desert, seashore and windblown sand
Irregular	Naturally irregular, or partly shaped by attrition and having rounded edges	Other gravels: land or dug flint
Flaky	Material of which the thickness is small relative to the other two dimensions	Laminated rock
Angular	Possessing well-defined edges formed at the intersection of roughly planar faces	Crushed rocks of all types
Elongated	Material, usually angular, in which the length is considerably larger than the other two dimensions	
Flaky and elongated	Material having the length considerably larger than the width, and the width considerably larger than the thickness	

The shape of fine aggregate particles influences the mix properties (stability, workability, bitumen content, etc.), angular particles requiring more bitumen. Angular aggregate shape is desirable in bituminous mixtures. Neville mentioned about fine aggregate angularity as;

"Mixtures because better interlocking of aggregates is obtained but an objective method of measuring and expressing shape is not yet available despite attempts using measurement of the projected surface area and other geometrical approximations" (Neville, 1997).

The shape of coarse aggregate particle is concerned, equidimensional shape of particles is preferred because particles, which significantly depart from such a shape, have a larger surface area and pack in an anisotropic manner. Two types of particles, which depart from equidimensional shape, are of interest, elongated and flaky. The

elongated flaky particle tends to be oriented in one plane, which affects adversely the durability of HMA.

The mass of flaky and elongated particle expressed as a percentage of the mass of the sample is called the flakiness and elongation index. The classification is described in British Standards 812 (1989):

- A particle is flaky if its thickness (least dimension) is less than 0.6 times the mean sieve size of the size fraction;
- Similarly, a particle whose length (largest dimension) is more than 1.8 times the mean sieve size of the size fraction is said to be elongated.

The mean size is defined as the arithmetic mean of the sieve size on which the particle is just retained and the sieve size through which the particle just passes. The flakiness and elongation tests are useful for general assessment of aggregates but they don't adequately describe the particle shape (Neville, 1986).

2.3.3 Aggregate Surface Texture

The surface texture, also called surface roughness, of particles is the sum of their minute surface features (Dolar Mantuani, 1983). It is an inherent and specific property that depends on the texture, the structure, and the degree of weathering of the parental rock.

For Masad (2002), texture in an image is represented by the local variation in the pixel gray intensity values. Then wavelet theory is used for multi-scale analysis of textural variation on aggregate images. The original image is decomposed into low-resolution images by iteratively blurring the original image. As a result, images that contain information on fine intensity variation are obtained. The process could be repeated again with these images and texture quantification can be made at different scales. In this way, values for the coarser and finer texture of the sample can be obtained (Masad, 2002).

The classification of the surface texture is based on the degree to which the particle surfaces are polished or dull, smooth or rough. The type of roughness has also to be described. Surface texture depends on the hardness, grain size and pore characteristic of the parent material “hard, dense and fine-grained rocks generally having smooth surfaces” (Neville, 1997) as well as on the degree to which forces acting on the particle surface have smoothed or roughened it. Visual estimate of roughness is quite reliable but, in order to reduce misunderstanding, the classification of BS 812; Part 1; 1975 given in Table 2.2, should be followed.

Table 2.2 Surface Texture of Aggregates (British Standards 812, 1975).

Group Surface texture	Characteristic	Examples
Glassy	Conchoidal fracture	Black flint, vitreous slag
Smooth	Water-worn, or smooth due to fracture of laminted or fine-grained rock	Gravels, chert, Slate, marble, some rhyolites
Granular	Fracture showing more or less uniform rounded grains	Sandstone, oolite
Rough	Rough fracture of fine-or medium grained rock containing no easily visible crystalline constituents	Basalt, felsite, porphyry,limestone
Crystalline	Containing easily visible crystalline constituents	Granite, gabbro gneiss
Honeycombed	With visible pores and cavities	Brick, pumice, foamed slag, clinker, expanded clay

There is no recognized method of measuring the surface roughness. The shape and surface texture of aggregates influence considerably the strength of HMA the full role of shape and surface texture of aggregates in the development of HMA strength is not known, but possibly a rougher particle texture results in a larger adhesive force between the particles and the asphalt cement mix. Likewise. The

larger surface area of aggregate angular means that a larger adhesive force can be developed (Topal & Sengoz, 2005).

CHAPTER THREE
AGGREGATE ANGULARITY AND RELATION WITH PERFORMANCE OF HOT MIX ASPHALT

Asphalt mixtures have two major components: coarse aggregate and fine aggregate. Each component contributes to the performance of the mixture. However, careful planning is required to quantify the effect of one of the components because the effects of the other one may confound the results.

The properties of hot mix asphalt (HMA) are affected substantially by the characteristics of aggregates, including angularity, shape and surface texture.

“Aggregate angularity is one of the most important property that should be considered in the mix design of asphalt pavements to avoid premature pavement failure” (Oduroh et al., 2000; Topal, 2001).

“Generally, angular and rough textured aggregates produce higher quality HMA, than smooth and rounded aggregates” (Freeman et al., 1999). Physical and mineralogical properties of mineral aggregates, which provide load bearing ability of pavement, affect directly properties of mixture, workability of fresh mixture and performance of pavement. The more workable bituminous mixtures, the more compactable they are. simply compactable bituminous mixtures can rut easily and quickly under traffic. In contrast, mixtures with subordinate workability (harsh mixtures), are fewer prone to rutting below the wheel path happens under same traffic conditions. Because of this cause, in recent years highway engineers in the USA and some European countries choose less workable bituminous mixtures, which are durable to compact. Angularity of aggregate is the key factor to affect workability (Topal & Sengoz, 2005).

Proper selection of aggregates in HMA can minimize the potential for premature pavement failures such as rutting, stripping, and fatigue cracking.

NCHRP Report 4-19 (1997) stated that a cubical and angular aggregate particle shape for both coarse and fine aggregate is desirable for increased aggregate internal friction and improved rutting resistance (Oduroh et al., 2000) and also SHRP (1993) at the same manner states, “By specifying coarse and fine aggregate angularity SUPERPAVE seeks to achieve HMA with a high degree of internal friction and thus, high shear strength for rutting resistance”.

Many researchers (Hicks, 1970; Hicks & Monismith, 1971; Allen,1973; Allen & Thompson, 1974; Thom, 1988; Barksdale & Itani, 1989; Thom & Brown, 1989) have reported that crushed aggregate, having angular to subangular shaped particles, provides better load distribution properties and a higher resilient modulus than uncrushed gravel with sub rounded or rounded particles. A rough particle surface is also said to result in a higher resilient modulus. Barksdale and Itani (1989) investigated several types of aggregate and observed that the resilient modulus of the rough, angular crushed materials was higher than that of the rounded gravel by a factor of about 50% at low mean normal stress and about 25% at high mean normal stress. “Although increasing particle angularity and surface roughness could result in higher resilient modulus, (Hicks, 1970; Hicks and Monismith, 1971; Allen, 1973)”. Lateral resilient movements being controlled by interparticle contact condition. (Freeman, 1999).

Aggregate testing and characterization must be targeted to the fraction(s) of aggregate in a mix that will control the frictional performance. In general, coarse aggregate controls the frictional properties of asphalt mixtures, while fine aggregate controls the frictional properties of concrete mixes. Exceptions include fine-graded asphalt mixes, where fine aggregates are in larger abundance, and concrete mixes in which coarse aggregates are either intentionally exposed at the time of construction (exposed aggregate concrete, porous concrete) or will become exposed in the future (diamond grinding/grooving, surface abrading).

Various researches indicates that the following aggregate properties have a significant influence on pavement friction performance (Dahir and Henry, 1978; Kandhal and Parker, 1998; Folliard and Smith, 2003):

- Hardness
- Mineralogy (i.e., mineral composition and structure)
- Shape
- Texture
- Angularity
- Abrasion Resistance
- Polish Resistance
- Soundness

Aggregate hardness and mineralogy largely dictate the wear characteristics (i.e., durability, polish) of the aggregate. Aggregates that display the highest levels of long-term friction are typically composed of hard, strongly bonded, interlocking mineral crystals (coarse grains) embedded in a matrix of softer minerals (Henry, 2000). The differences in grain size and hardness provide a constantly renewed abrasive surface because of differential wear rates and the breaking off of the harder grains from the softer matrix of softer minerals.

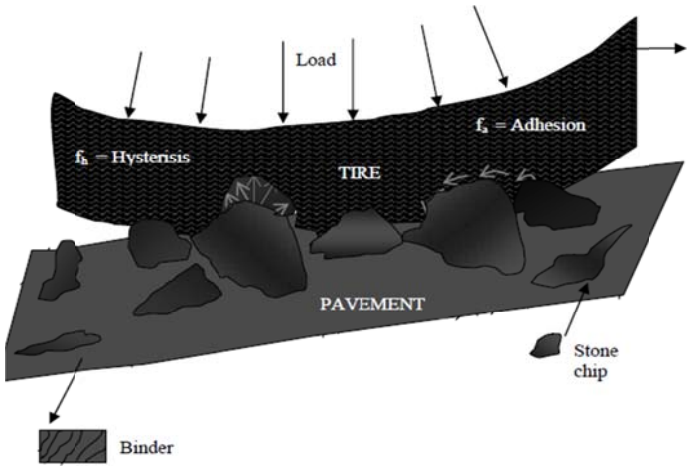

Figure 3.1 The relation between aggregate surface characteristics and pavement friction.

3.1 Fine Aggregate Angularity

It has long been documented that the characteristics of the fine aggregate component of HMA can have a major and sometimes dominant influence on mixture rutting and fatigue cracking resistance (Topal. A, Sengoz. B, 2005). Kandhal et al. (1999) have classified the test methods to describe the aggregate angularity into two broad categories; direct and indirect. Direct methods are defined as those wherein particle shape or texture are measured and described qualitatively or quantitatively through direct measurement of individual particles. In indirect methods, particle shape and texture are determined based on measurements of bulk properties.

Similar to the previous researches fine aggregate angularity doesn't have any effect on the surface properties, such as surface texture and friction, of HMA (Hall, 2006). The role of fine aggregate becomes significant only when used in relatively large quantities (Shupe, 1960).

Hall et al. performed an exclusive study that relates fine aggregate angularity characteristics with micro texture. Their research indicated that fine aggregates that exhibit angular edges and cubical or irregular shapes generally provide higher levels of micro-texture, whereas those with rounded edges or elongated shapes generally produce lower micro-texture (Hall, 2006).

Fine aggregate angularity determination in the thesis includes EN 933-6 (AFNOR P18-564) and ASTM C1252 (AASHTO TP33). The details regards to the performance of the tests will be explained in further chapters in detail.

3.2 Coarse Aggregate Angularity

Coarse aggregate characteristics (angularity and texture) are believed to have a significant role in pavement surface properties such as friction and texture.

The desired texture is attained and retained by use of hard, irregularly shaped coarse aggregate. Hard, polish-resistant coarse aggregate is essential to avoid reducing skid resistance of asphalt surface (Bloem, 1971). Common causes of friction loss include polishing of coarse aggregates and excessive wearing of the pavement surface resulting in a loss of macro-texture.

The resistance of an aggregate type against polishing is the key factor in pavement surface properties. The use of polish-resistant coarse aggregates or other aggregates with good frictional performance has always been considered a useful way to have passable pavement surface properties.

Coarse aggregate angularity determination in the thesis includes modified ASTM C1252 (AASHTO TP 56), ASTM D4791 and BS 812. The details regards to the performance of the tests will be explained in further chapters in detail.

CHAPTER FOUR
CRUSHERS

4.1 Crushing Process

Crushing is the first mechanical stage in the process of comminution in which the main objective is the liberation of the valuable minerals from the gangue. It is generally a dry operation and is usually performed in two or three stages. Lumps of runof- mine ore can be as large as 1.5 m across and these are reduced in the primary crushing stage to 10-20 cm in heavy-duty machines.

In most operations, the primary crushing schedule is the same as the mining schedule. When primary crushing is performed underground, this operation is normally a responsibility of the mining department; when primary crushing is on the surface, it is customary for the mining department to deliver the rock to the crusher and for the mineral processing department to crush and handle the rock from this point through the successive rock processing unit operations. Primary crushers are commonly designed to operate 75 % of the available time, mainly because of interruptions caused by insufficient crusher feed and by mechanical delays in the crusher (Lewis et al., 1976; Topal, 2001)

Secondary crushing includes all operations for reclaiming the primary crusher product from rock storage to the disposal of the final crusher product, which is usually between 0.5 and 2 cm in diameter. The primary crusher product from most metalliferous rocks can be crushed and screened satisfactorily, and the secondary plant generally consists of one or two size-reduction stages with appropriate crushers and screens. If, however, the rock tends to be slippery and tough, the tertiary crushing stage may be substituted by coarse grinding in rod mills.

Vibrating screens are sometimes placed ahead of the secondary crushers to remove undersize material, or scalp the feed, and thereby increase the capacity of the secondary crushing plant. Undersize material tends to pack the voids between the large particles in the crushing chamber, and can choke the crusher, causing damage, because the packed mass of rock is unable to swell in volume as it is broken.

4.2 General Classification of Crushers:

Crushers are classified into two as (Wills, 1984):

Primary Crushers:

- Jaw Crushers
- Gyratory Crushers

Secondary Crushers:

- Jaw Crushers
- Gyratory Crushers
- Cone Crushers
- Impact Crushers
- Roll Crushers

4.2.1 Primary Crushers

Primary crushers are heavy-duty machines, used to reduce the run-of-mine ore down to a size suitable for transport and for feeding the secondary crushers. They are always operated in open circuit, with or without heavy-duty scalping screens. There are two main types of primary crusher in metalliferous operations –jaw and gyratory crushers- although the impact crusher has limited use as a primary crusher and will be considered separately. Figure 4.1 shows the open circuit and closed circuit crushing.

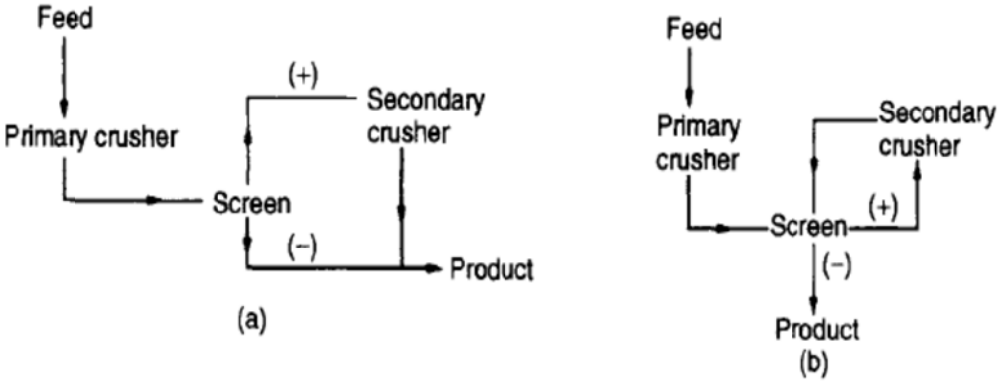

Figure 4.1 (a) Open-circuit crushing, (b) closed-circuit crushing (Wills, 1984).

4.2.1.1 Jaw Crushers

The distinctive feature of this class of crusher is the two plates which open and shut like animal jaws (Grieco & Grieco, 1985). The jaws are set at an acute angle to each other, and one jaw is pivoted so that it swings relative to the other fixed jaw. Material fed into the jaws is alternately *nipped* and released to fall further into the crushing chamber. Eventually it falls from the discharge aperture. A typical view of Jaw crusher is performed in Figure 4.2.

Jaw crushers are designed to impart an impact on a rock particle placed between a fixed and a moving plate (jaw). The faces of the plates are made of hardened steel. Both plates could be flat or the fixed plate flat and the moving plate convex. The surfaces of both plates could be plain or corrugated. The moving plate applies the force of impact on the particles held against the stationary plate. Both plates are bolted on to a heavy block. The moving plate is pivoted at the top end (Blake crusher) or at the bottom end (Dodge-type crusher) and connected to an eccentric shaft. In universal crushers the plates are pivoted in the middle so that both the top and the bottom ends can move (Figure 4.3).

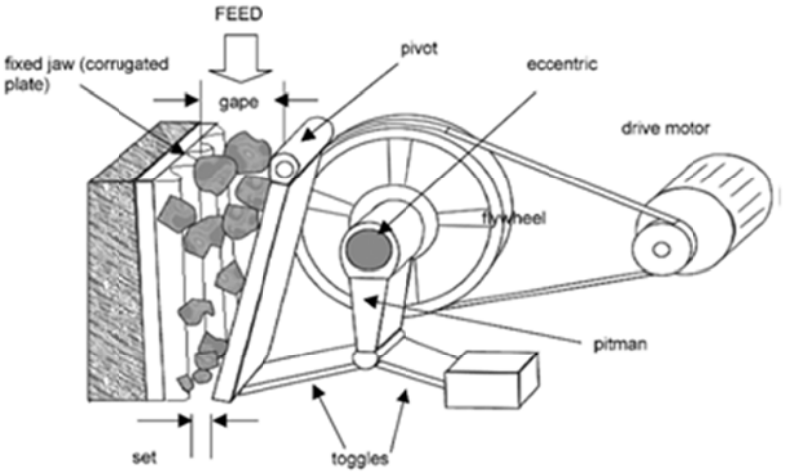

Figure 4.2 Jaw crusher

Jaw crushers range in size up to 1680 mm gape by 2130 mm width. This size machine will handle ore with a maximum size of 1.22 m at a crushing rate of approximately 725th^{-1} with a 203mm set. However, at crushing rates above 545 th^{-1} the economic advantage of the jaw crusher over the gyratory diminishes; and above 725 th^{-1} jaw crushers cannot compete with gyratory crushers (Lewis, 1976).

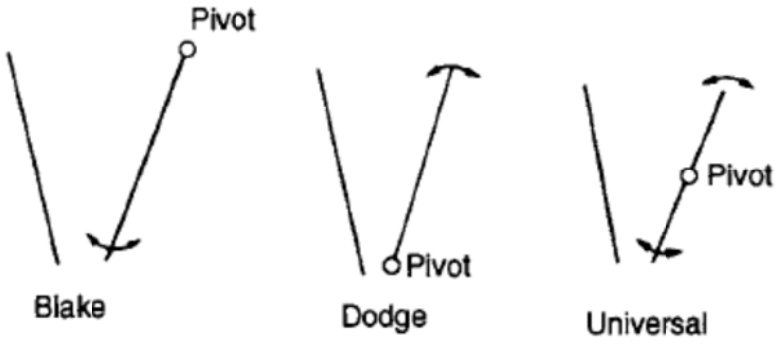

Figure 4.3 Jaw crusher types

4.2.1.2 Gyratory Crushers

Gyratory crushers are principally used in surfacecrushing plants, although a few currently operate underground. The gyratory crusher (Figure 4.4) consists essentially of a long spindle, carrying a hard steel conical grinding element, the head, seated in an eccentric sleeve. The spindle is suspended from a "spider" and, as it rotates,

normally between 85 and 150 rev min^{-1}, it sweeps out a conical path within the fixed crushing chamber, or shell, due to the gyratory action of the eccentric. As in the jaw crusher, maximum movement of the head occurs near the discharge. This tends to relieve the choking due to swelling, the machine thus being a good arrested crusher. The spindle is free to turn on its axis in the eccentric sleeve, so that during crushing the lumps are compressed between the rotating head and the top shell segments, and abrasive action in a horizontal direction is negligible.

Primary crushers are solidly built to receive large lumps of rock directly from the mines and designed for large tonnage throughputs. Basically gyratory crushers consist of a fixed solid conical shell or bowl (also called concaves) and a solid cone within the bowl called a breaking head (Figure 4.4). The breaking head is fixed to a central spindle, which is hydraulically suspended or mechanically held from a spider. The bottom end of the spindle usually rests on a hydraulically supported piston. The bottom end of the spindle is connected to a bevel and pinion arrangement with straight or spiral teeth which on rotating by a journal moves the bottom of the shaft eccentrically. In some models, the spindle is fixed at the top and bottom and is made to move side-ways to impart the crushing action. The entire assembly can be visualised as a circular jaw crusher.(Wills, 1999; Topal, 2001)

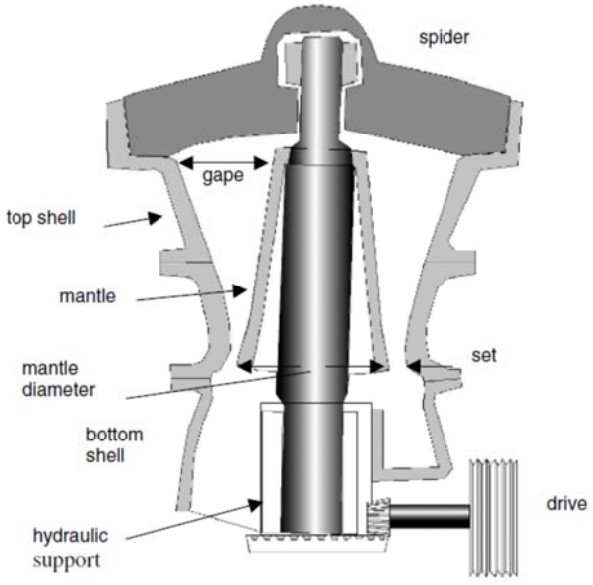

Figure 4.4 Gyratory Crusher Functional Diagram

4.2.2 Secondary Crushers

Secondary crushers are much lighter than the heavy-duty, rugged primary machines. Since they take the primary crushed ore as feed, the maximum feed size will normally be less than 15 cm in diameter and, because most of the harmful constituents in the ore, such as tramp metal, wood, clays, and slimes have already been removed, it is much easier to handle. Similarly, the transportation and feeding arrangements serving the crushers do not need to be as rugged as in the primary stage. Secondary crushers also operate with dry feeds, and their purpose is to reduce the ore to a size suitable for grinding. In those cases where size reduction can be more efficiently carried out by crushing, there may be a tertiary stage before the material is passed to the grinding mills.

4.2.2.1 The Cone Crusher

The cone crusher is a modified gyratory crusher. The essential difference is that the shorter spindle of the cone crusher is not suspended as in the gyratory, but is supported in a curved, universal bearing below the gyratory head or cone" (Wills, 1984).

Power is transmitted from the source to the countershaft through a V-belt or direct drive. The countershaft has a bevel pinion pressed and keyed to it, and drives the gear on the eccentric assembly.

The eccentric has a tapered, offset bore and provides the means whereby the head and main shaft follow an eccentric path during each cycle of rotation. Since a large gape is not required, the crushing shell or "bowl" flares outwards which allows for the swell of broken ore by providing an increasing cross-sectional area towards the discharge end. The cone crusher is therefore an excellent arrested crusher. The flare of the bowl allows a much greater head angle than in the gyratory crusher, while retaining the same angle between the crushing members.

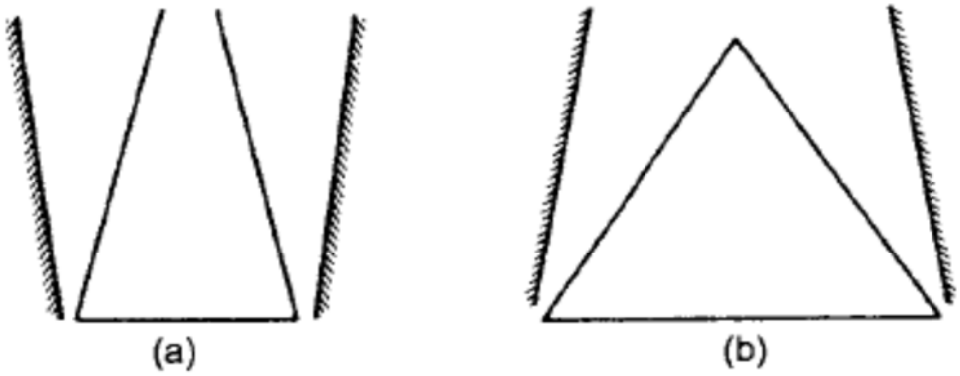

Figure 4.5 Head and Shell Shapes of (a) Gyratory, and (b) Cone Crushers

While, retaining the same angle between the crushing members (Figure 5.8).This gives the cone crusher a high capacity, since the capacity of gyratory crushers is roughly proportional to the diameter of the head.

An important feature of the crusher is that the bowl is held down either by an annular arrangement of springs or by a hydraulic mechanism. These allow the bowl to yield if 'tramp' material enters the crushing chamber so permitting the offending object to pass. If the springs are continually 'on the work' as may happen with ores containing many very tough particles oversize material will be allowed to escape from the crusher. This is one of the reasons for using closed circuit crushing in the final stages. It may be necessary to choose a screen for the circuit, which has apertures slightly larger than the set of the crusher. This is to reduce the tendency for very tough particles, which are slightly oversize to 'spring' the crusher causing an accumulation of such particles in the closed circuit and a buildup of pressure in the crushing throat.

4.2.2.2 Gyradisc Crushers

The gyradisc crusher is a specialized form of come crusher used for producing fine material.

“The main modification to the conventional cone crusher is that the machine has very short liners and a very flat angle for the lower liner. Crushing is by interparticle comminution by the impact and attrition of a multi-layered of particle.

The angle of the lower liner is less than the angle of repose of the ore so that when the liner is at rest the material does not slide. Transfer through the crushing zone is by movement of the head. Each time the lower liner moves away from the upper liner material enters the attrition chamber from the surge load above.

When reduction begins material is picked up by the lower liner and is moved outward. Due to the slope of the liner it is carried to an advanced position and caught between the crushing members.

The length of stroke and the timing are such that after the initial stroke the lower liner is withdrawn farter than the previously crushed material falls by gravity. This permits the lower liner to recede and return to strike the previously crushed mass as it is falling, thus scattering it so that a new alignment of particles is obtained prior to another impact. At each withdrawal of the head the void is filled by particles from the surge chamber.” (Wills, 1984)

At no time does single-layer crushing occur, as with conventional crushers. Crushing is by particle on particle so that the setting of the crusher is not as directly related to the size of product, as it is cone crusher (Topal, 2001).

Their main use is in quarries for producing sand and gravel. When used in open circuit they will produce a product of chipping from about 1 cm downward of good cubic shape with a satisfactory amount oft sand, which obviates the use of blending and rehandling. In closed circuit they are used to produce large quantities of sand. They may be used in open circuit on clean metalliferous ores with no primary slimes to produce an excellent ball-mill feed. Minus-19mm material may be crushed to about 3 mm.

4.2.2.3 Roll Crushers

Roll crushers consist of two or more adjacent rolls placed parallel to each other and rotated in opposite directions. Single roll crushers are also available which rotate a single roll against a fixed breaker plate. Mineral or rock particles placed between the rolls are nipped and then crushed as they pass between the rolls. Rolls are held against each other by springs. Radical changes to the design of roll crushers have been introduced by Schonert, as a result of fundamental work on breakage mechanisms. These roll crushers have large forces of compression and are called High Pressure Grinding Rolls (HPGR).

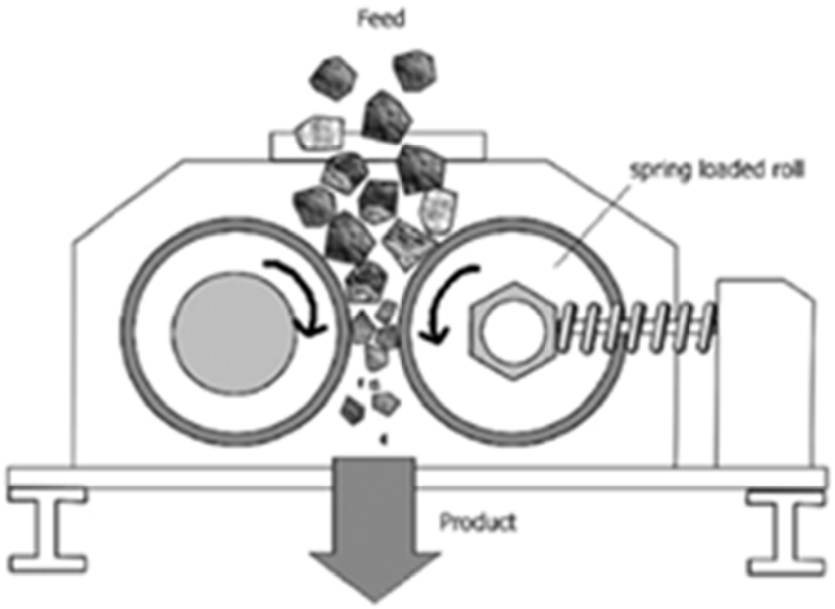

Figure 4.6 Roll crusher

Unlike jaw and gyratory crushers, where reduction is progressive by repeated pressure as the material passes down to the discharge point, the crushing process in rolls is one of single pressure.

Two types of roll crushers are generally designed. In the first type both rolls are rigidly fixed to a frame with provision for adjusting the lateral position of one of the rolls to control the gap between them. Once set these rolls are locked into place. One roll is attached to the driving mechanism while the other rotates by friction. Single roll crushers are also available which rotate a single roll against a fixed breaker plate.

In the second type, at least one roll is spring mounted which forms the driving roll; the other roll rotates by friction (Fig.4.6).

The nest of springs helps to provide uniform pressure along the length of the rolls. The springs are helical and pressure varies with the size of crusher and could be as high as 6 t/meter (about 8300 kPa).

In some roll crushers the rolls are individually driven. The drive is either by gears or belt. Both rolls usually rotate at the same speed but some crushers are designed such that one roll could rotate faster than the other. For fine grinding both rolls are rigidly fixed to the base and therefore they do not permit any movement of the rolls during operation. The surfaces of the rolls are smooth, corrugated or ribbed. Heavy duty toothed rollers are sometimes used as primary crushers but the use of such rollers in the metallurgical industry is very limited.

Some rollers are toothed. The shape of the teeth is generally pyramidal. The roll surfaces play an important part in the process of nipping a particle and then dragging it between the rolls. The corrugated and ribbed surfaces offer better friction and nip than smooth surfaced rolls. The toothed surfaces offer additional complex penetrating and compressive forces that help to shatter and disintegrate hard rock pieces.

The distance between the rolls is adjusted by nuts at the end of one of the rolls. The nip angle is affected by the distance between the rolls. The nip angle is defined as the angle that is tangent to the roll surface at the points of contact between the rolls and the particle. It depends on the surface characteristics of the rolls. Usually the nip angle is between 20° and 30° but in some large roll crushers it is up to 40°.

4.2.2.4 Impact Crusher

In this class crusher comminution is by impact rather than compression by sharp blows applied at high speed to free-falling rock. The moving parts are beaters, which transfer of their kinetic energy to the ore particles on contacting them. The internal

stresses created in the particles are often large enough to cause them to shatter (Figure 4.7).

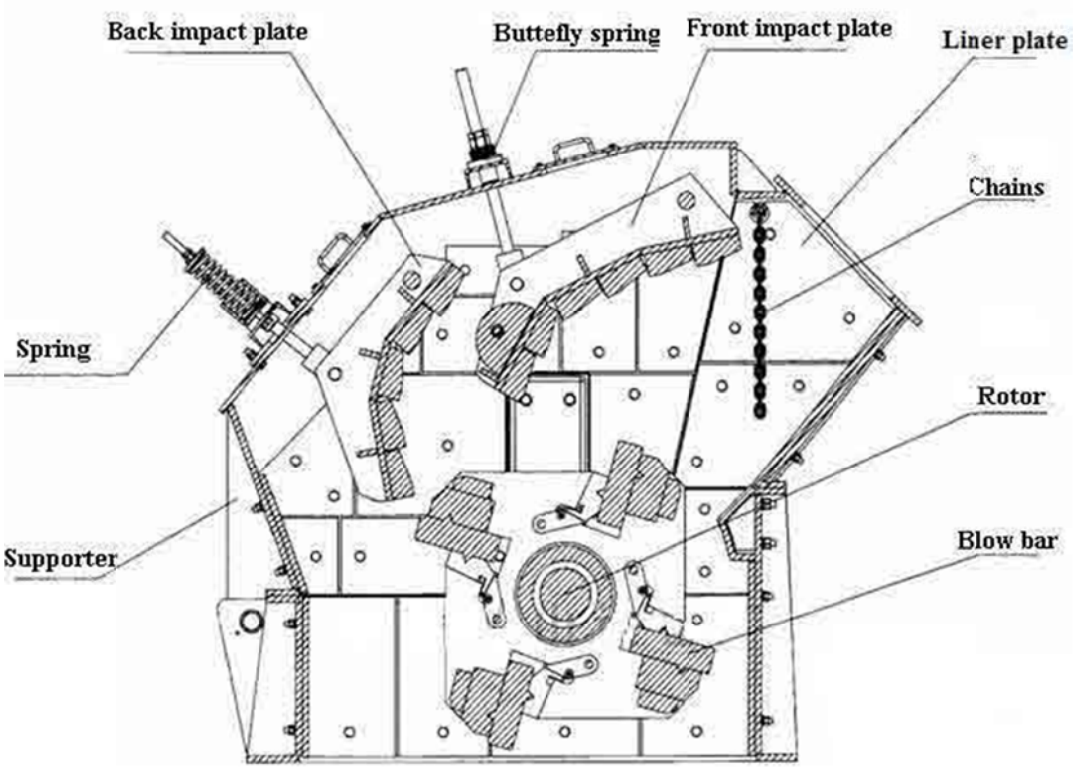

Figure 4.7 Impact Crusher Functional Diagram

Causing the particles to impact upon an anvil or breaker plate increases these forces. There is an important difference between the states of materials crushed by pressure and by impact. There are internal stresses materials broken by pressure, which can cause later cracking. Impact causes immediate fracture with no residual stresses. This stress-free condition is particularly valuable in stone used for brick making, building, and road-making, in which binding agents, such as bitumen are subsequently added to the surface. Impact crushers; therefore have a wider use in the quarrying industry than in the metal-mining industry.

They may give trouble-free crushing on ores that tend to be plastic and pack when the crushing forces are applied slowly, as is the case in jaw and gyratory crushers. These types of ore tend to be brittle when the crushing force is applied instantaneously by impact crushers. (Wills, 1984; Topal, 2001)

The crushers used in this thesis include Impact crusher, Jaw crusher and Roll crusher.

CHAPTER FIVE
PAVEMENT SURFACE PROPERTIES

This section summarizes the general knowledge, and the research studies that have been done on characterization of the frictional properties of the pavement surface.

5.1 Pavement Surface Texture

Pavement surface texture is defined as the deviations of the pavement surface from a true planar surface. These deviations occur at three distinct levels of scale, each defined by the wavelength (λ) and peak-to-peak amplitude (*A*) of its components (Figure 5.1). The profile of the surface is described by its displacement along the surface and its displacement in the direction normal to the surface. The former is called distance and the latter is called amplitude here. The distance may be in a longitudinal or lateral (transverse) direction in relation to the direction of travel, or any direction between these. Texture wavelength is defined as the (minimum) distance between periodically repeated parts of the curve in its direction along the surface plane.

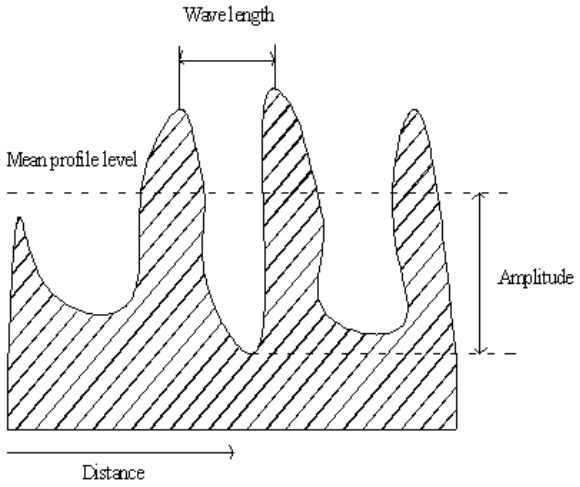

Figure 5.1 Representation of surface texture characteristics.

The three levels of texture, as established in 1987 by the Permanent International Association of Road Congresses (PIARC), are as follows:

- Micro-texture ($\lambda < 0.02$ in [0.5 mm], A = 0.04 to 20 mils [1 to 500 μm]) Surface roughness quality at the sub-visible or microscopic level. It is a function of the surface properties of the aggregate particles contained in the asphalt or concrete paving material.
- Macro-texture (λ = 0.02 to 2 in [0.5 to 50 mm], A = 0.005 to 0.8 in [0.1 to 20 mm]) Surface roughness quality defined by the mixture properties (shape, size, and gradation of aggregate) of asphalt paving mixtures and the method of finishing/texturing (dragging, tining, grooving; depth, width, spacing and orientation of channels/grooves) used on a concrete paved surfaces.
- Mega-texture (λ = 2 to 20 in [50 to 500 mm], A = 0.005 to 2 in [0.1 to 50 mm]) Texture with wavelengths in the same order of size as the pavement–tire interface.

It is largely defined by the distress, defects, or “waviness” on the pavement surface. Wavelengths longer than the upper limit (20 in [500 mm]) of mega-texture are defined as roughness or unevenness (Henry, 2000). Figure 5.1 illustrates the three texture ranges, as well as a fourth level roughness/unevenness—representing wavelengths longer than the upper limit (20 in [500 mm]) of mega-texture.

It is widely recognized that pavement surface texture influences many different pavement tire interactions. Figure 5.2 shows the ranges of texture wavelengths affecting various vehicle–road interactions, including friction, interior and exterior noise, splash and spray, rolling resistance, and tire wear. As can be seen, friction is primarily affected by microtexture and macro-texture, which correspond to the adhesion and hysteresis friction components, respectively.

Pavement surface characteristics classification and their impact on pavement performance measurements are presented in Figure 5.3.

Figure 5.4 shows the relative influences of micro-texture, macro-texture, and speed on pavement friction. As can be seen, micro-texture influences the magnitude of tire friction, while macro-texture impacts the friction–speed gradient. At low speeds, micro-texture dominates the wet friction level. At higher speeds, the presence of high macro-texture facilitates the drainage of water so that the adhesive component of friction is re-established. Hysteresis increases with speed exponentially, and at speeds above 65 mil/hr (105 km/hr) could account for over 95 percent of the friction (Rado et al., 2006).

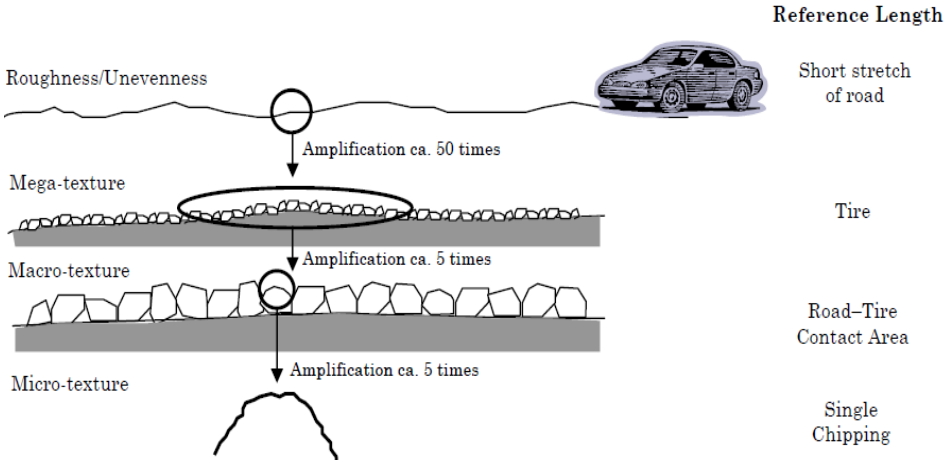

Figure 5.2 Simplified illustrations of the various texture ranges that exist for a given pavement surface (Sandburg, 1998).

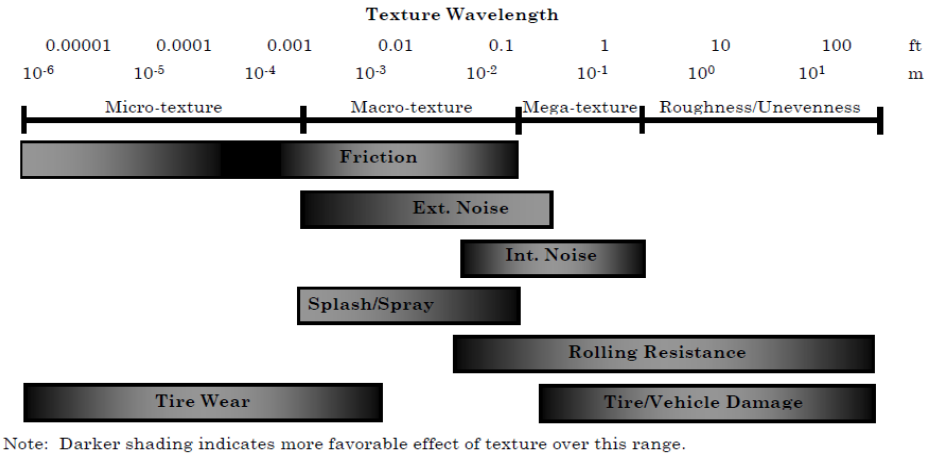

Figure 5.3 Texture wavelength influence on pavement tire interactions (Henry, 2000; Sandburg and Ejsmont, 2002).

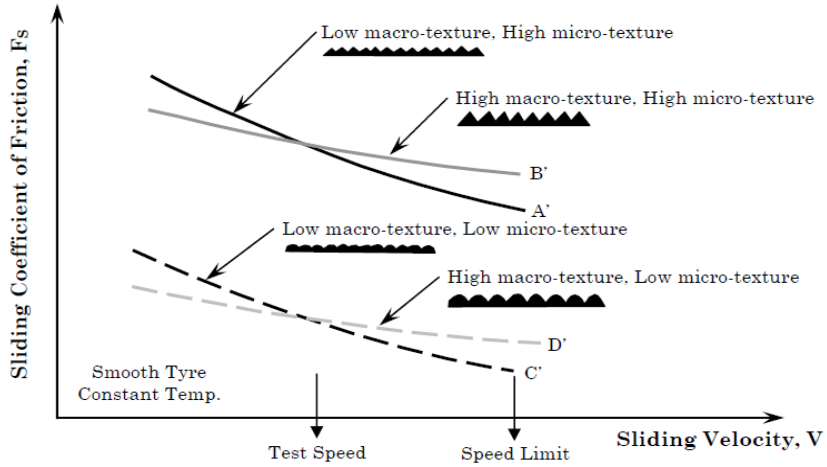

Figure 5.4 Effect of microtexture and macrotexture on pavement tire friction at different sliding speeds (Flintsch et al., 2002).

In addition, it is deemed necessary to define some of the texture measures which will be essential for this section. These definitions are as follows:

- Texture Depth: In the three-dimensional case, the term texture depth (TD) means the average distance, within a certain surface area in the same order of a size as that of a tire/road interface, between the surface and a plane through the top of the three highest particles 'well spaced' within the surface area.

- Mean Texture Depth: In the application of the 'Volumetric Patch Method' (see above) the 'plane' is in practice determined by the contact between a rubber pad and the surface when the pad is rubbed over the area. Therefore, the texture depth obtained in this case is not exactly a 'plane' but rather an approximation that is somewhat curved and hard-to-define surface. The texture depth obtained in the case of the volumetric patch method is called mean texture depth (MTD).

- Mean Profile Depth: mean profile depth (MPD) means the average difference, within a certain longitudinal/lateral distance in the same order of a size as that of a tire/road interface, between the profile and a line through the top of the highest particle within the profile sample considered.

5.1.1 Factors Affecting Surface Texture

The factors that affect pavement surface texture, which relate to the aggregate, binder, and mix properties of the surface material and any texturing done to the material after placement, are as follows:

- Maximum Aggregate Dimensions: The size of the largest aggregates in asphalt concrete (AC) or exposed aggregate PCC pavement will provide the dominant macrotexture wavelength, if closely and evenly spaced.
- Coarse Aggregate Type: The selection of coarse aggregate type will control the stone material, its angularity, its shape factor, and its durability. This is particularly critical for AC and exposed aggregate PCC pavements.
- Fine Aggregate Type: The angularity and durability of the selected fine aggregate type will be controlled by the material selected and whether it is crushed.
- Binder Viscosity and Content: Binders with low viscosities tend to cause bleeding more easily than the harder grades. Also, excessive amounts of binder (all types) can result in bleeding. Bleeding results in a reduction or total loss of pavement surface micro-texture and macro-texture. Because binder also holds the aggregate particles in position, a binder with good resistance to weathering is very important.
- Mix Gradation: Gradation of the mix, particularly for porous pavements, will affect the stability and air voids of the pavement.
- Mix Air Voids: Increased air content provides increased water drainage to improve friction and increased air drainage to reduce noise.
- Layer Thickness: Increased layer thickness for porous pavements provides a larger volume for water dispersal. On the other hand, increased thickness reduces the frequency of the peak sound absorption.
- Texture Dimensions: The dimensions of PCC tining, grooving, grinding, and turf dragging affect the macro-texture, and therefore the friction and noise.

- Texture Spacing: Spacing of transverse PCC tining and grooving not only increases the amplitude of certain macro-texture wavelengths, but can affect the noise frequency spectrum.
- Texture Orientation: PCC surface texturing can be oriented transverse, longitudinal, and diagonally to the direction of traffic. The orientation affects tire vibrations and, hence, noise.
- Isotropic or Anisotropic: Consistency in the surface texture in all directions (isotropic) will minimize longer wavelengths, thereby reducing noise.
- Texture Skew: Positive skew results from the majority of peaks in the macrotexture profile, while negative skew results from a majority of valleys in the profile.

Table 5.1 Factors Affecting Pavement Micro Texture and Macro Texture (Sandberg, 2002; Henry, 2000; Rado, 1994; PIARC, 1995; AASHTO, 1976)

Pavement surface type	Factor	Micro texture	Macro texture
Asphalt	Minimum aggregate dimension		■
	Coarse aggregate types	■	■
	Fine aggregate types		■
	Mix gradation		■
	Mix air content		■
	Mix binder		■
Concrete	Coarse aggregate type	■	■
	Fine aggregate types	■	
	Mix gradation		■
	Texture dimension and spacing		■
	Texture orientation		■
	Texture skew		■

Table 5.1 provides a summary of how these factors influence micro-texture and macrotexture. These factors can be optimized to obtain pavement surface characteristics required for a given design situation.

5.1.2 Texture Measurement Methods

The measurement of pavement texture has been of primary importance for the last 50 years. Many different types of equipment have been developed and used to measure the pavement surface texture properties, and their differences (in terms of measurement principles and procedures and the way measurement data are processed and reported) can be significant.

Texture measuring equipment requiring lane closures include the sand patch method (SPM) (ASTM E 965), the outflow meter (OFM) (ASTM E 2380), circular texture meter (CTM) (ASTM E 2157) and 3D laser scanner method (ASTM E 1845-01). In the thesis, both sand-patch and 3D laser scanner methods have been applied. The details of these experimental procedures will be explained in Section 6.5.1 and 6.5.2.

The sand patch method is a volumetric-based spot test method that assesses pavement surface macrotexture through the spreading of a known volume of glass beads in a circle onto a cleaned surface and the measurement of the diameter of the resulting circle. The volume divided by the area of the circle is reported as the mean texture depth (MTD).

The OFM is a volumetric test method that measures the water drainage rate through surface texture and interior voids. It indicates the hydroplaning potential of a surface by relating to the escape time of water beneath a moving tire. The equipment consists of a cylinder with a rubber ring on the bottom and an open top. Sensors measure the time required for a known volume of water to pass under the seal or into the pavement. The measurement parameter, outflow time (OFT), defines the macro-texture; high OFTs indicating smooth macro-texture and low OFTs rough macro-texture.

The CTM is a non-contact laser device that measures the surface profile along an 11.25in (286mm) diameter circular path of the pavement surface at intervals of 0.034

in (0.868 mm). The texture meter device rotates at 20 ft/min (6 m/min) and generates profile traces of the pavement surface, which are transmitted and stored on a portable computer. Two different macro-texture indices can be computed from these profiles mean profile depth (MPD) and root mean square (RMS). The MPD, which is a two-dimensional estimate of the three-dimensional MTD (Flintsch et al., 2003), represents the average of the highest profile peaks occurring within eight individual segments comprising the circle of measurement.

Also advances in laser technology and computational power have led to the development of systems that measure pavement longitudinal profile at highway travel speeds. The data from these systems can be used to compute the mean profile depth (MPD).

High-speed methods for characterizing pavement surface texture are typically based on non-contact surface profiling techniques. An example of a non-contact profiler for use in characterizing pavement surface texture is the Road Surface Analyzer (ROSANV), developed by the FHWA. ROSANV is a portable, vehicle-mounted, automated system for the measurement of pavement texture at highway speeds along a linear path. ROSANV incorporates a laser sensor mounted on the vehicle's front bumper and the device can be operated at speeds of up to 70 mi/hr (113 km/hr). The system calculates both MPD and estimated mean texture depth (EMTD), which is an estimate of MTD derived from MPD using a transformation equation.

5.2 Pavement Surface Friction

5.2.1 Introduction to Friction

Pavement friction is the force that resists the relative motion between a vehicle tire and a pavement surface. This resistive force, illustrated in Figure 5.5, is generated as the tire rolls or slides over the pavement surface (Rado, 2006).

Pavement friction plays a vital role in keeping vehicles on the road, as it gives drivers the ability to control/maneuver their vehicles in a safe manner, in both the longitudinal and lateral directions. It is a key input for highway geometric design, as it is used in determining the adequacy of the minimum stopping sight distance, minimum horizontal radius, minimum radius of crest vertical curves, and maximum super-elevation in horizontal curves. Figure 5.5 presents the diagram of forces acting on a rotating wheel.

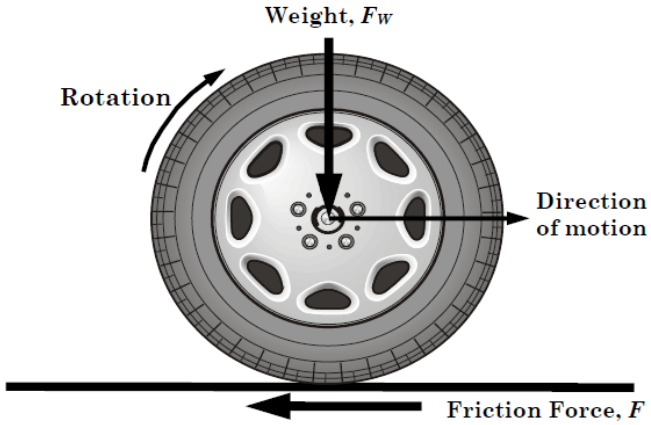

Figure 5.5 Simplified diagram of forces acting on a rotating wheel.

5.2.2 Friction Mechanism

Pavement friction is the result of a complex interplay between two principal frictional force components adhesion and hysteresis (Figure 5.6). Adhesion is the friction that results from the small-scale bonding/interlocking of the vehicle tire rubber and the pavement surface as they come into contact with each other. It is a function of the interface shear strength and contact area.

The hysteresis component of frictional forces results from the energy loss due to bulk deformation of the vehicle tire. The deformation is commonly referred to as enveloping of the tire around the texture. When a tire compresses against the pavement surface, the stress distribution causes the deformation energy to be stored within the rubber. As the tire relaxes, part of the stored energy is recovered, while the

other part is lost in the form of heat (hysteresis), which is irreversible. That loss leaves a net frictional force to help stop the forward motion.

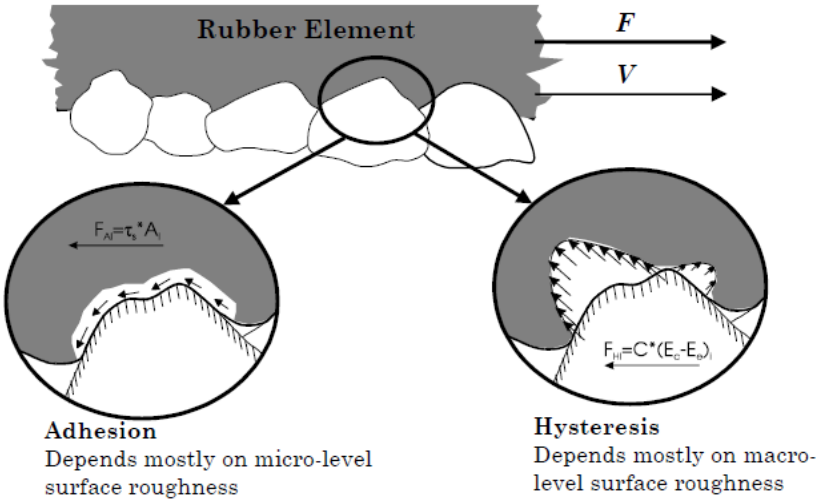

Figure 5.6 Key mechanisms of pavement–tire friction.

Although there are other components of pavement friction (e.g., tire rubber shear), they are insignificant when compared to the adhesion and hysteresis force components. Thus, friction can be viewed as the sum of the adhesion and hysteresis frictional forces.

$$F = Fa + Fh \qquad [5.1]$$

Both components depend largely on pavement surface characteristics, the contact between tire and pavement, and the properties of the tire. Also, because tire rubber is a visco-elastic material, temperature and sliding speed affect both components.

Because adhesion force is developed at the pavement–tire interface, it is most responsive to the micro-level asperities (micro-texture) of the aggregate particles contained in the pavement surface. In contrast, the hysteresis force developed within the tire is most responsive to the macro-level asperities (macro-texture) formed in the surface via mix design and/or construction techniques. As a result of this phenomenon, adhesion governs the overall friction on smooth-textured and dry

pavements, while hysteresis is the dominant component on wet and rough-textured pavements.

5.2.3 Factors Affecting Surface Friction

The factors that influence pavement friction forces can be grouped into four categories pavement surface characteristics, vehicle operational parameters, tire properties, and environmental factors. Table 5.2 lists the various factors comprising each category. Because each factor in this Table plays a role in defining pavement friction, friction must be viewed as a process instead of an inherent property of the pavement. It is only when all these factors are fully specified that friction takes on a definite value.

The more critical factors are shown in bold in Table 5.2 and are briefly discussed below. Among these factors, the ones considered to be within a highway agency's control are microtexture and macro-texture, pavement materials properties, and slip speed.

Table 5.2 Factors affecting available pavement friction (wallman and astrom, 2001)

Pavement surface characteristics	Vehicle operating parameters	Tire properties	Environment
• **Micro texture** • **Macro texture** • Mega texture • **Material properties** • Temperature	• **Slip speed** • Vehicle speed • Breaking action • Driving maneuver • Turning • overtaking	• Foot print • **Tread design and condition** • Rubber composition and hardness • **Inflation pressure** • Load • temprature	• Climate • Wind • **Temperature** • **Water (rainfall, condensation** • **Snow and ice** • **Contaminants** • Anti skid material (salt, sand)

❖ Note: critical factors are shown in bold

5.2.4 Friction measurement methods

The two devices commonly used to measure pavement friction characteristics in the laboratory or at low speeds in the field are the British Pendulum Tester (BPT) (AASHTO T 278 or ASTM E 303) and the Dynamic Friction Tester (DFT) (ASTM E 1911). Both these devices measure frictional properties by determining the loss in

kinetic energy of a sliding pendulum or rotating disc when in contact with the pavement surface. The loss of kinetic energy is converted to a frictional force and thus pavement friction. These two methods are highly portable and easy to handle. The DFT has the added advantage of being able to measure the speed dependency of the pavement friction by measuring friction at various speeds (Saito et al., 1996). The details of the experimental procedure related to DFT and BPT will be explained in chapter 6.5.3 and 6.5.4.

High-speed friction measurements utilize one or two full-scale test tires to measure pavement friction properties in one of four modes: locked-wheel, side-force, fixed-slip, or variable slip. As noted by Henry (2000) and confirmed by the state survey conducted in this study, the most common method for measuring pavement friction in the U.S. is the locked wheel method (ASTM E 274). This method is meant to test the frictional properties of the surface under emergency braking conditions for a vehicle without anti-lock brakes. Unlike the side-force and fixed-slip methods, the locked-wheel approach tests at a slip speed equal to the vehicle speed, this means that the wheel is locked and unable to rotate (Henry, 2000).

The results of the locked-wheel test are reported as a friction number (*FN,* or skid number [*SN*]). Locked-wheel friction testers usually operate at speeds between 40 and 60 mi/hr (64 and 96 km/hr). Testing can be done using a smooth (ASTM E 524) or ribbed tire (ASTM E 501).

The ribbed tire is insensitive to the pavement surface water film thickness; thus it is insensitive to the pavement macro-texture. The smooth tire, on the other hand, is sensitive to macro-texture.

The side-force method (ASTM E 670) measures the ability of vehicles to maintain control in curves and involves maintaining a constant angle, the yaw angle, between the tire and the direction of motion.

Since the yaw angle is typically small, between 7.5 and 20°, the slip speed is also quite low; this means that side-force testers are particularly sensitive to the pavement micro-texture but are generally insensitive to changes in the pavement macro-texture.

The two most common side-force measuring devices are the Mu-Meter and the Side-Force Coefficient Road Inventory Machine (SCRIM). The primary advantage offered by side-force measuring devices is the ability for continuous friction measurement throughout a test section (Henry, 2000). This ensures that areas of low friction are not skipped due to a sampling procedure.

Fixed-slip devices measure the friction experienced by vehicles with anti-lock brakes. Fixed-slip devices maintain a constant slip, typically between 10 and 20 percent, as a vertical load is applied to the test tire (Henry, 2000).

CHAPTER SIX
EXPERIMENTAL

The research undertaken in this chapter examines the relationship between the aggregate properties such as angularity and pavement surface characteristics such as texture and friction.

The consequences will be used to recommend a technique for the assortment of aggregate types and crushers used in asphalt pavement surface to ensure acceptable surface properties.

6.1 Materials

This section includes the presentation of the detailed properties of materials used within the experiments.

6.1.1 Aggregate

As it was mentioned in the literature review, aggregate type and mineralogical properties of aggregate have a significant effect on the surface properties of the pavement. Three different types of aggregates were selected:

- Limestone
- Basalt
- and mixture of limestone and basalt (basalt constitutes the coarse aggregate portion where as the Limestone constitutes the fine aggregate portion).

Natural Limestone aggregates were procured from Dere Beton/Izmir quarry. For the related aggregate types, in order to clearly evaluate the effect of aggregate type and crusher, only one type of gradation-dense gradation-is chosen. Grading of aggregate was chosen in conformity with the Type 1 wearing course of Turkish Specifications. Table 6.1 presents the aggregate gradation board.

Table 6.1 Aggregate gradation board

Sieve Size/No.	Specification	Gradation (%) and results	Specification limits
3/4”	ASTM C 136	100	100
1/2”		92	83–100
3/8”		80.5	70–90
No 4		47.3	40–55
No 10		33.0	25–38
No 40		13.5	10–20
No 80		9.0	6–15
No 200		5.3	4–10

Natural Basalt aggregates were also procured from Aliaga/Izmir pit. The properties of the Limestone and Basalt aggregates are presented in Table 6.2. Table 6.3 presents different aggregate and crusher types utilized for preparing each sample.

Table 6.2 The properties of Limestone and Basalt aggregate

Specific gravity (coarse aggregate)	Specification	Limestone	Basalt	Specification limits
Bulk	ASTM C 127	2.686	2.666	
SSD		2.701	2.810	
Apparent		2.727	2.706	
Specific gravity (fine aggregate)				
Bulk	ASTM C 128	2.687	2.652	
SSD		2.703	2.770	
Apparent		2.732	2.688	
Specific gravity (filler)		2.725	2.731	-
Los Angeles abrasion (%)	ASTM C 131	22.6	14.2	Max 30
Sodium sulphate soundness (%)	ASTM C 88	1.47	2.6	Max 10-20

Table 6.3 Aggregate and crushers type for each sample

Aggregate type	Crusher type	Aggregate sample name	Slab name
Limestone	Impact crusher	LIA	LIP
Limestone	Jaw crusher	LJA	LJP
Limestone	Roll crusher	LRA	LRP
Basalt	Impact crusher	BIA	BIP
Basalt	Jaw crusher	BJA	BJP
Mixture of basalt and limestone	Impact crusher	MIA	MIP
Mixture of basalt and limestone	Jaw crusher	MJA	MJP
Mixture of basalt and limestone	Roll crusher	MRA	MRP

6.1.2 Bitumen

The bitumen with a 50/70 penetration grade was procured from Aliaga/Izmir Oil Terminal of the Turkish Petroleum Refinery Corporation. In order to characterize the properties of the base bitumen, conventional test methods such as: penetration test, softening point test, ductility, and test were performed. These tests were conducted in conformity with the relevant test methods that are presented in Table 6.4.

Table 6.4 Results properties of base bitumen

Test	**Specification**	**Results**	**Specification limits**
Penetration (250 °C; 0.1 mm)	ASTM D5 EN 1426	55	50-70
Softening point (°C)	ASTM D36 EN 1427	49.1	46-54
Viscosity at (135°C)-Pa.s	ASTM D4402	412.5	-
TFOT (163 °C; 5h)	ASTM D1754 EN 12607-1	137.5	-
Change of mass (%)		0.04	0.5 (max)
Retained penetration (%)	ASTM D5 EN 1426	25	-
Ductility (25°C)-cm	ASTM D113	100	-
Specific gravity	ASTM D70	1.030	-
Flash point (°C)	ASTM D92 EN 22592	260	230 (min)

6.2 Aggregate Characterization

This section includes the determination of coarse and fine aggregate angularity as well as flat & elongated particles and flakiness index.

6.2.1 Fine Aggregate Angularity Test Methods

There are two standardized test methods for fine aggregate angularity: EN933-6 (AFNOR P18-564) and ASTM C1252 (AASHTO TP33) methods. These methods are presented below.

6.2.1.1 EN 933-6 (AFNOR P18-564)

EN 933-6 was published by AFNOR in 1990 (TS EN 933-6, 2006). The aim of the specification is to define the procedure to measure flow rate of fine aggregate. This specification has an application area on natural or processed sand used in civil engineering. Flow rate of fine aggregates of a given volume is defined as the flow time in seconds through an orifice under specified conditions. Figure 6.1 presents the flow rate test apparatus:

Figure 6.1 Flow rate test Apparatus (Verstraeten, 1994).

Tests performed using 0.08 – 2 mm (No.200-No.10) or 0.08 - 4 mm (No.200-No.5) sized sand samples. Mass in terms of kg of the sample, is given by Pr/2.7 relation. For 0.08 – 2 mm sized fine aggregate, the funnel with 12 mm orifice is used, for 0.08 - 4 mm sized coarser fine aggregate, the funnel with 16 mm orifice is employed. Openings are closed with mobile shutter. Sample is placed into the funnel.

Chronometer is started by the time of the mobile shutter is opened. The materials start to flow into the pan and flow time for the total material flow is measured with 1/10 second precision. The test is repeated at least five times with the same materials.

6.2.1.2 ASTM C1252 (AASHTO TP33)

ASTM C1252 standard test method based on the technical substance provided by the Strategic Highway Research Program (SHRP) researchers. This standard was collected and formatted jointly by the AASHTO and SHRP staffs. (AASHTO, 1993)

Standard test method is designated for uncompacted void content of fine aggregate as influenced by particle shape, surface texture and grading. This method describes the determination of the loosely uncompacted void content of a sample fine aggregate. When measured on any aggregate of a knowing grading, void content provides an indication of aggregate's angularity, sphericity and surface texture compared with other fine aggregates tested in same grading. Figure 6.2 shows the picture of the fine aggregate angularity apparatus:

Figure 6.2 Fine aggregate angularity (ASTM C1252) apparatus

Three procedures are utilized for the measurement of void content. Two utilize graded fine aggregate (standard grading or as-received grading), and the other uses several individual size fractions for void content determinations:

Standard Graded Sample (Method A): This method uses a standard fine aggregate grading that is obtained by combining individual sieve fractions from a typical fine aggregate sieve analysis. See the section on Preparation of Test Sample for the grading. Standard Graded Sample-weigh out and combine the following quantities of fine aggregate which has been dried and sieved in accordance with Test Method ASTM C136. For each of the following size fractions shows in Table 6.5:

Table 6.5 size fractions for each sample.

Individual Size Fraction	Mass, g
2.36-mm (No.8) to 1.18-mm (no. 16)	44
1.18-mm (No.16) to 600- μm (No.30)	57
600- μm (No.30) to 300- μm (No.50)	72
300- μm (No.50) to 150- μm (No.100)	17

*The tolerance on each of these amounts is ± 0.2 g.

Individual Size Fractions (Method B): This method uses each of three fine aggregate size fractions: (a) 2.36 mm (No.8) to 1.18mm (No.16); (b) 1.18-mm (No.16) to 600-µm (No.30); and (c) 600-µm (No.30) to 300-µm (No.50). For this method each size is tested separately. Individual Size Fractions-Prepare a separate 190-g sample of fine aggregate, dried and sieved in accordance with Test Method C136, for each of the following size fractions shows in Table 6.6:

Table 6.6 size fractions for each sample.

Individual Size Fraction	Mass, g
2.36-mm (No.8) to 1.18-mm (no. 16)	190
1.18-mm (No.16) to 600- µm (No.30)	190
600- µm (No.30) to 300- µm (No.50)	190
300- µm (No.50) to 150- µm (No.100)	190

*The tolerance on each of these amounts is ± 1 g. Each size is tested separately.

As-Received Grading (Method C): This method uses that portion of the fine aggregate finer than a 4.75 mm (No.4) sieve. (AASTHO TP33, 1993) Obtain a 190 g sample of the material passing the 4.75-mm (No. 4) sieve for test. This process is not included in the scope of the study.

A nominal 100-mL calibrated cylindrical measure is filled with fine aggregate of prescribed grading by allowing the sample to flow through a funnel from a fixed height into the measure. The fine aggregate is struck off, and its mass is determined by weighing. Uncompacted void content is calculated as the difference between the volume of the cylindrical measure and the absolute volume of the fine aggregate collected in the measure. Uncompacted void content is calculated using the bulk dry specific gravity of the fine aggregate. Two runs are made on each sample and the results are averaged (AASTHO TP33, 1993).

The uncompacted voids are calculated for each determination by the following equation (6.1):

$$U = \frac{V - (\frac{F}{G})}{V} X\,100 \qquad [6.1]$$

Where:

V = volume of cylindrical measure, mL

F = net mass, g, of fine aggregate in measure (Gross mass minus the mass of the empty measure).

G = bulk dry specific gravity of fine aggregate.

U = uncompacted voids, percent, in the material. (AASHTO TP33, 1993)

6.2.2 Coarse Aggregate Angularity Test Methods

Coarse aggregate angularity determination uses modified ASTM C1252 (AASTHO TP56).

The void content of coarse aggregate measurement provides an indication of angularity, sphericity and surface texture compared to other aggregates of the same grading. Uncompacted void content is computed as the difference between the volume of the cylindrical measure and the absolute volume of the coarse aggregate collected (Based on bulk dry specific gravity as determined by AASHTO T85).

Higher void content in samples of equal size gradation by this procedure indicate, a combination of greater angularity or less sphericity. Figure 6.3 illustrates the apparatus used for coarse aggregate angularity.

AASHTO TP·56 provides three methods of void content measurement, the differences in method differs by the type of sample used: (AASHTO TP 56, 2003)

- Method A: Sample of standard grading is made up from several specified gradations in specific masses totaling 5000g.
- Method B: Separate 5000g samples are tested for each of three sieve Gradations and then averaged.

- Method C: An as-received 5000g sample is used, taken after removing material finer than the #4 (4.75mm) sieve. This method is not included in the scope of the study.

Figure 6.3 coarse aggregate angularity apparatus

The uncompacted void content is determined by the following equation:

$$U = \frac{V - (\frac{F}{G})}{V} X\,100 \qquad [6.2]$$

Where:

V = volume of cylindrical measure, ml

F = net mass of coarse aggregate in measure, g

G = bulk dry specific gravity of coarse aggregate

(By AASHTO T85 procedure)

U = uncompacted voids, percent in the material

6.2.3 Flat &Elongated Particles and Flakiness Index Test Methods

The section involves the determination of flat and elongated particles as well as flakiness index.

6.2.3.1 Flat and Elongated Particles Test Method

The flat and elongated particle test is used to determine the dimensional ratios for aggregate particles of specific sieve sizes. This characterization is used in the Superpave specification to identify aggregate that may have a tendency to impede compaction or have difficulty meeting VMA specifications due to aggregate degradation. Flat or elongated particles (Figure 6.4) tend to lock up more readily (rather than reorient) during compaction making compaction more difficult. They also have a tendency to fracture during compaction along their weak, narrow dimension, which can effectively make aggregate gradation finer and possibly cause lower-than-expected VMA. Figure 6.4 (a) and (b) presents flat and elongated particle aggregate sample and the caliper device used for the test respectively.

Figure 6.4 (a) Flat particles (left) and elongated particles (right). (b) Calipers device for the flat and elongated particle test

The percentage of flat and elongated particles in each size fraction is determined by the following equation:

$$Pi = \frac{F}{T} X 100 \qquad [6.3]$$

Where:

Pi = percent flat & elongated of individual size fraction

F = mass of flat and elongated particles in fraction

T = total mass of particles in fraction

6.2.3.2 B.S. 812 (Flakiness Index)

This method is included in British Standards. This method is based on the classification of aggregate particles as flaky when they have a thickness (smallest dimension) of less than 0.6 of their nominal size, this size being taken as the mean of the limiting sieve apertures used for determining the size fraction in which the particle occurs. The flakiness Index of an aggregate sample is found by separating the flaky particles and expressing their mass as a percentage of the mass of the sample tested. The test is not applicable to material passing a 6.30 mm BS test sieve or retained on a 63.0 mm BS test sieve. Figure 6.5 shows the flakiness index test method apparatus:

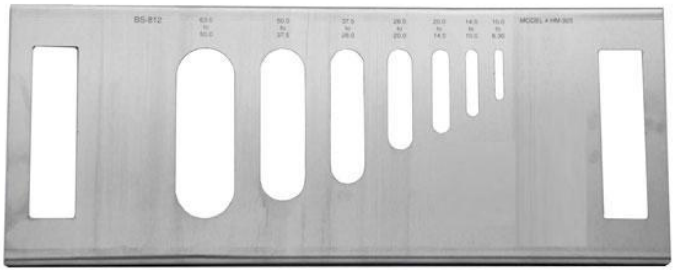

Figure 6.5 BS 812 apparatus for flakiness index

All aggregates retained on the 63.0 mm BS test sieve and all aggregate passing the 6.30 mm BS test sieve is first discarded. Each of the individual size-fractions retained on the sieves weighed and stored them in separate trays with their size marked on the trays.

Where the number of particles in any size fraction is considered to be excessive more than the appropriate mass, the fraction may be subdivided by standard methods. Under such circumstances the rest of the procedure should be suitably modified and

the appropriate correction factor applied to determine the mass of flaky particles that would have been obtained had the whole of the original size-fraction been gauged.

From the sums of the masses of the fractions in the trays (M_1), the individual percentages retained on each of the various sieves have been calculated. Any fraction of which the mass is 5% or less of mass M_1 Discarded and remaining mass has recorded (M_2). Select the thickness gauge appropriate to the size fraction under test and each particle tested separately by hand. All the passing particles weighed and recorded (M_3).

The Flakiness Index shall be reported to the nearest whole number. The sieve analysis obtained in the test shall also be reported. Calculate the percentage of flaky particles in each size fraction to the nearest 0.1% according to the equation shown below (6.4):

$$\text{Flakiness Index} = \frac{M3}{M2} \times 100 \qquad [6.4]$$

6.3 Optimum Bitumen Content Determination by Marshall Method

The concept of the Marshall method of mix design was originally conceived by Mr. Bruce Marshall, formerly a bituminous engineer with the Mississippi State Highway Department. The Marshall method was later further improved by the U.S. Corps of Engineers who added certain features and developed the mix design criteria. The Marshall Mix design method and criteria were originally developed for airfield pavements, but were later also adopted for use in highway pavements. Due to its simplicity, the Marshall method of mix design was the most commonly used mix design method in the U.S. before the introduction of the Superpave design system, and it is still the most commonly-used mix design methods in the rest of the world.

The Marshall mix design procedure as recommended by the Asphalt Institute is described in detail in the Manual “Mix Design Methods for Asphalt Concrete and

Other Hot-Mix Types" by the Asphalt Institute (1997). The Marshall mix design procedure consists of the following main elements:

1. Selection of aggregates: The aggregates must meet all the requirements as specified by the local highway agency. These requirements typically include limits on L.A. abrasion loss, soundness loss, sand equivalent, percent of deleterious substance, percent of natural sand, percent of particles with crushed faces, and percent of flat or elongated particles. The gradation of the aggregate blend to be used must meet the gradation requirements for dense-grade HMA mixture as set by the local highway agency.

2. Selection of bitumen: The bitumen must meet the specification requirements as set by the local highway agency.

3. Preparation of asphalt mixture samples: Samples of asphalt mixtures at five different bitumen contents, with three replicates per bitumen content are prepared. The bitumen contents are selected at 0.5% increments with at least two bitumen contents above the estimated optimum and at least two below it. The aggregate and bitumen are mixed at a temperature at which the bitumen kinematic viscosity is 170 ± 20 centistokes.

4. Compaction of the asphalt mixtures: The asphalt mixture is compacted in a 101.6-mm (4-inch) diameter cylindrical mold by a Marshall compaction hammer, which is 4.5 kg (10 pounds) in weight and dropped from a height of 457 mm (18 inches) for a specified number of blows per side of the specimen. The number of blows to be applied per side is 35, 50 or 75 for light, medium or heavy designed traffic, respectively. Light traffic is defined as having less than 10^4 ESALs. Medium traffic has between 10^4 and 10^6 ESALs, while heavy traffic has more than 10^6ESALs. Compaction of the mixtures is done at a temperature at which the asphalt kinematic viscosity is 280 ± 20 centistokes. The compacted specimen is 101.6 mm (4 inches) in diameter and approximately 63.5 mm (2.5 inches) in height.

5. Testing of the compacted Marshall specimens: The tests to be run on the Marshall specimens include (1) determination of bulk specific gravity in accordance with AASHTO T166 (2004) or ASTM D2726 (2004) and (2) Marshall stability test, which measures the Marshall stability and Marshall flow, in accordance with ASTM D1559 (2004). The Marshall stability is the maximum load the specimen can withstand before failure when tested in the Marshall stability test. The configuration of the Marshall stability test is close to that of the indirect tensile strength test, except for the confinement of the Marshall specimen imposed by the Marshall testing head. Thus, the Marshall stability is related to the tensile strength of the asphalt mixture. The Marshall flow is the total vertical deformation of the specimen, in units of 0.01 inch, when it is loaded to the maximum load in the Marshall stability test. The Marshall flow can provide some indication of the resistance of an asphalt mixture to plastic deformation. Mixtures with low Marshall flow numbers are stiff and may be difficult to compact. However, these mixtures are more resistant to rutting than those with high flow numbers. Mixtures with Marshall flow numbers above the normal range may be "tender mixes", which are susceptible to permanent deformation.

6. Computation of volumetric properties of the specimens - Using the bulk specific gravity of the specimen, the maximum specific gravity of the mixture and the bulk specific gravity of the aggregate, the percent air voids and VMA of the specimen are determined.

7. Marshall mix design criteria: The Marshall mix design method as recommended by the Asphalt Institute uses five mix design criteria. They are (1) a minimum Marshall stability, (2) a range of acceptable Marshall flow, (3) a range of acceptable air voids, (4) percent voids filled with asphalt (VFA), and (5) a minimum amount of VMA. Table 1 shows the requirements for stability, flow, air voids and VFA.

8. Determination of design asphalt content: To facilitate the selection of optimum asphalt content, the following six plots are made:

- Average unit weight versus asphalt content
- Average air voids versus asphalt content

- Average Marshall stability versus asphalt content
- Average Marshall flow versus asphalt content
- Average VMA versus asphalt content
- Average VFA versus asphalt content

Table 6.7 presents the Marshall Mix Design Requirements on Stability, Flow, Air Voids and VFA .

Table 6.7 Marshall Mix Design Requirements on Stability, Flow, Air Voids and VFA (Mix Design Methods for Asphalt Concrete and Other Hot-Mix Types, Asphalt Institute 1997)

Traffic Category	Light		Medium		Heavy	
Compaction, No. of blows/side	35		50		75	
Stability (kgf)	Min.	Max.	Min.	Max.	Min.	Max.
	400	-	600	-	900	-
Flow (mm)	2	4.5	2	4	2	4
Air Voids, %	3	5	3	5	3	5
VFA, %	65	75	65	78	65	75

6.4 Preparation of Slabs

Regarding to the mix designs, one of gradation dense graded is used. In order to evaluate the aggregate angularity different crushers are used. The optimum bitumen content was also determined for each of the sample and used in preparation of test specimens.

In the thesis, one slab designates one mixture type and the related utilized crusher. Aggregates of each mix were blended and split into two buckets for heating. The HMA mix weight was calculated to produce a 5cm (2 in.) thick slab given the mold volume and bulk specific gravity. The buckets containing aggregates were put into the oven one night before compaction at the mixing temperature. The bitumen was also split into beakers can to achieve uniform heating. The small cans of desired asphalt type were also heated to their mixing temperature. The heated aggregate was

weighed, and the optimum asphalt content was added to it and placed in the mixer for each one of the mixtures.

The two steel buckets of aggregate to make up the total batch were placed in a 170°C oven overnight. This temperature and time was chosen to assure a constant temperature throughout the aggregate before mixing. For each of the mixtures, a 60 second mixing time was applied to the aggregate and fiber blend prior to adding bitumen to have a consistent mixture. The mixing was performed in a "bucket type" laboratory mixer. In each sample, mixing continued to assure a consistent mix with a uniform asphalt film thickness around each particle. During the mixing time, a spatula was used to aid the mixing process and scratch off any fines and asphalt from the side of the container. This process helped to obtain a uniform mix with minimum segregation and total number of uncoated aggregate (Vollor and Hanson, 2006).

After mixing, the mixture samples were placed into an oven in separate batches, and the mixes were conditioned for two hours at the compaction temperature (150°C) according to the AASHTO R 30 (2002) specification.

A metal mold was fabricated to impound the mixture during the compaction. This mold consists of five metal pieces bolted together and forms a frame to confine the mixture. In this form, an 80cm x 80cm base plate is underlying four 7cm x 7cm sections as the walls. One ramp-shape metal piece were also fabricated and mounted at the end of the frame to facilitate moving of the walk-behind roller compactor up to the frame. Figure 6.6 depicts a picture of the mold used to impound the mixture during compaction.

Figure 6.6 Picture of the Mold Used in Slab Compaction

After mixing, the mixture was transported to the compacting area in the metal buckets and spread inside the frame, being uniformly distributed. The HMA was then pushed out to the corners and smoothed out using trowel. This process was performed fast and carefully to provide a smooth surface with minimum segregation and temperature loss (Vollor and Hanson, 2006). Specimens were compacted using the walk-behind roller at their compaction temprature (145-150°C). Compaction process can be seen in Figure 6.7. Each sample was 65cm (26 inches) in side and approximately 5cm (2 inches) in thick.

Figure 6.7 Compacting Process

6.5 Test methods related to surface texture and skid resistance

There are many methods developed to measure texture and skid resistance properties of a pavement so far. Methods and the associated tests used in this study are mostly based on ASTM standards. These methods are accordingly, the Sand patch test method (ASTM E965, 1998) to measure mean texture depth (MTD), a recent and more reliable LASER Scanner (ASTM E 1845-01,2003) to obtain mean profile depth (MPD), Dynamic Friction Tester (ASTM E 1911-98, 1999) used to measure the friction coefficient of a surface at a regular speed (0 – 90 Km/hr) and British Pendulum Tester (ASTM E 303, 2002).

6.5.1 Sand Patch Test Method

This standard describes the test procedure for carrying out the sand patch test in order to measure the texture of a surface. The test is undertaken on any dry surface with spreading a known quantity of sand or any particulate fine grain materials with uniform gradation, e.g., glass beads on the surface. The material is then evenly distributed over a circular area to bring it flush with the highest aggregate peaks.

The diameter of the circle is measured in four different angles evenly spaced and averaged. By knowing the test material volume (24.6 ml) and diameter of the circle, the mean texture depth could easily be calculated (Eq 6.5). Figure 6.8 depicts the sand patch test being performed on an asphalt slab.

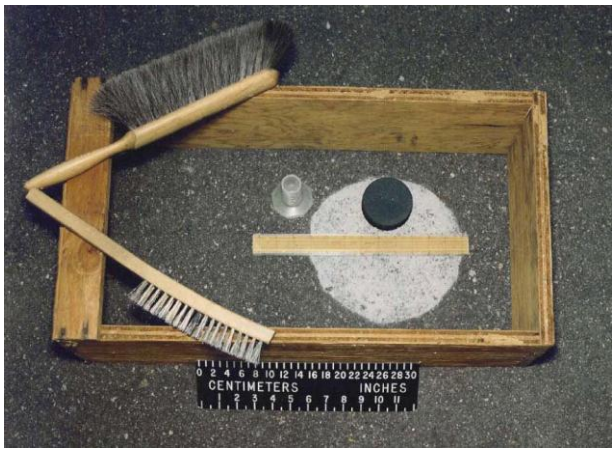

Figure 6.8 Photo of volumetric texture depth (sand patch) test equipment with glass beads.

$$\mathrm{MTD} = \frac{4.\mathrm{V}}{\pi.\mathrm{D}^2 \mathcal{AVG}} \qquad [6.5]$$

Where;

V = the exact volume of glass sphers, ml

D= Average diameter of sand patch in, mm

6.5.2 3D Laser Scanning

Since the volumetric method (sand patch test) is impractical, slow and has poor repeatability, the work has been initiated with the aim to develop an alternative measurement device to the sand patch test. Improvements of measuring devices in recent years make the measurement techniques faster and more reliable. New data acquisition techniques include interferometry, terrestrial laser scanner that acquires three dimensional spatial data, as well as various 2D and 3D profiling methods with new calibration techniques and the Scanning Laser Position Sensor (SLPS).

In this study, the Metris Model Maker D100 3D laser scanner (class 2M) including enhanced sensors was utilized to inspect full range of colors and depths on the selected asphalt pavement surfaces. The laser equipment was mounted on a portable vehicle attached to a computer as presented in Fig. 6.9. The Model Maker D with true digital camera technology includes several groundbreaking innovations such as second generation Enhanced Sensor Performance (ESP2). This device provides a better tradeoff between resolution and efficiency in texture data collection.

As shown in Fig. 6.9, the device measures texture by means of laser light. Laser intensity output is controlled by the processing unit to maintain a constant level of light on the detector. The possible angle of incidence will depend on the measured material and on the surface geometry. The sensor consists of a light source and a detector integrated with optics and electronics. It is insensitive to ambient light. When the light source projects a beam to hit a pavement surface, a scattered

reflection will occur. This light spot on the surface is viewed by a camera mounted inside the sensor. Depending on the distance between the laser head and the measured spot, the image of the light spot will be reflected to focus on a certain position on the detector. As the resolution depends on the range to the object, in the field studies the scanners' enhanced sensor was established to provide an optimum resolution of 15μm in the lateral direction and an optimum resolution of 10μm in the vertical direction.

Figure 6.9. 3D LASER scanning test device

The other important measure of the usefulness of the laser scanner is the accuracy (bias). This parameter determines how well the data represent the actual geometry of the scanned scene of object. For the 3D laser scanner utilized, the accuracy is expressed in terms of standard deviation of the ten measurements made on the same test surface. The standard deviation related to the calibration surface was found as 0.04 mm.

The Model Maker D is capable of sampling 1000 texture elevation points across a 100mm wide laser line at 150 Hz as it scans the road surface at about 0.1m/s. More importantly, the result is a 3D texture profile along a 100mm wide swath of pavement surface. The laser scanner adapts its laser power to suit the surface characteristics of pavement through enhanced scanning performance. During scanning process, laser device automatically tracks changes based on the surface conditions (both color and reflectivity of the bitumen as well as some minerals) parallel to the direction of the moving traffic and adapts laser power and sensor settings. Fig. 6.10 exhibits the different textured surfaces taken by the 3D laser scanner.

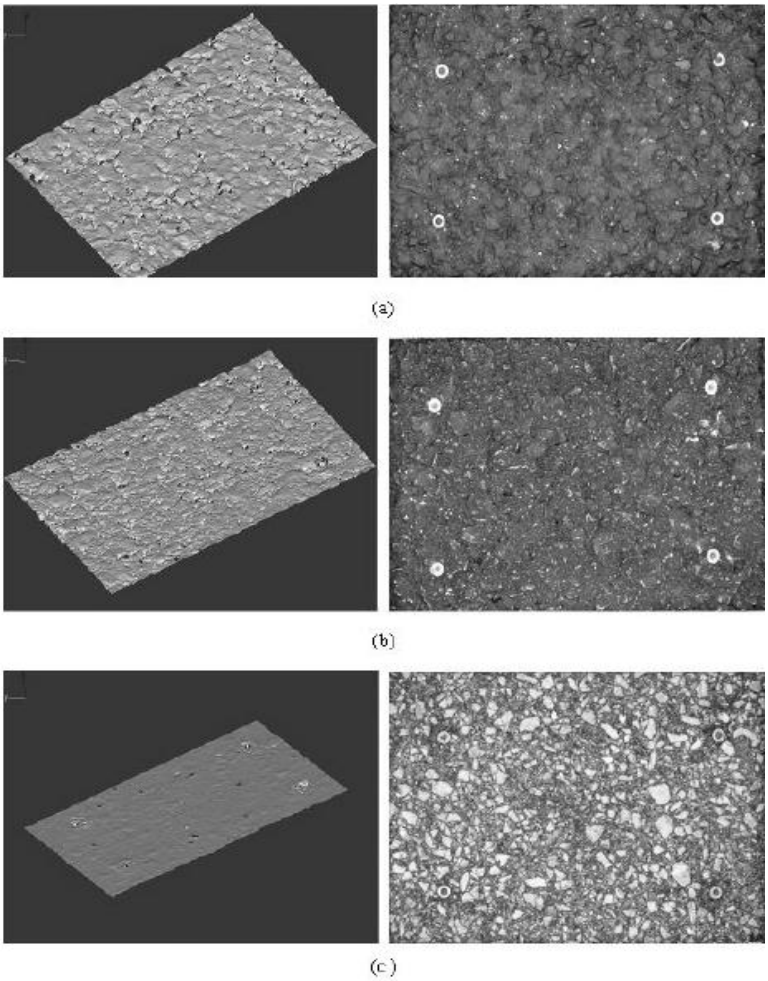

Figure 6.10 The images of different textured asphalt pavement surfaces (laser scanned images on left-images captured by 12.1 Mp CCD camera on right).

The surfaces scanned with the Model Maker D were also captured by 12.1 Mp CCD camera as illustrated in Figure 6.10. The Model Maker D laser scanner are also supplied with a data acquisition software (Kube) which is integrated and specifically designed for capturing and processing the laser stripe data. Following the acquisition procedure of the set of surface (Fig. 6.11 (a)) and cross-section (Fig. 6.11 (b)) of pavement samples with Kube software, it is necessary to characterize them with appropriate indicators such as mean profile depth (MPD).

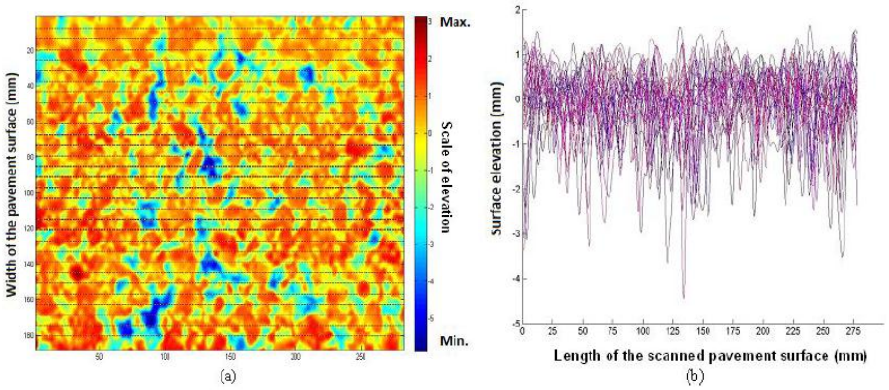

Figure 6.11 The profile and a cross section example of an asphalt pavement surface.

Based on descriptions given in ASTM E 1845 standard, before computing the MPD, the surface profile was filtered by applying a low pass filter in order to remove wavelengths 2.5mm followed by suppressing the profile slope by subtracting a regression line from the profile. The MPD was computed from a sample baseline divided into two equal half as presented in Fig. 6.12. The peak level in each half was determined and the average of the two peaks was termed as MPD.

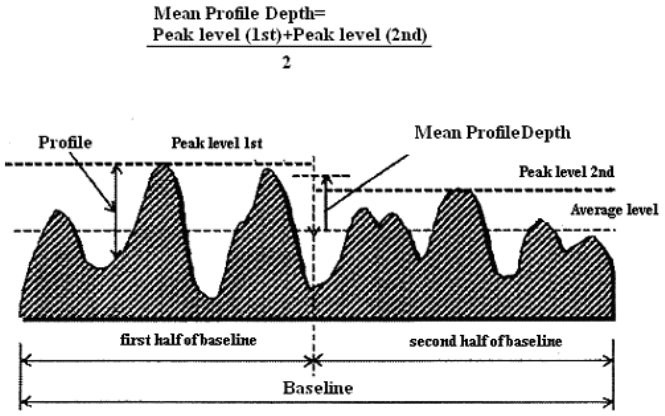

Figure 6.12. Standard method used for calculating MPD

6.5.3 *Dynamic Friction Tester*

The Dynamic Friction Tester as described by ASTM E 1911 consists of three rubber sliders and a motor that reaches to 100 km/h tangential speed. The rubber sliders are attached to a 350 mm circular disk by spring-like supports that facilitate the bounce back of the rubber sliders from the pavement surface. The test is started while the rotating disk is suspended over the pavement and driven by a motor to a particular tangential speed. The disk is then lowered, and the motor is disengaged. In the meantime, water is sprayed on the rubber and pavement interface through surrounding pipes to simulate wet weather friction. By measuring the traction force in each rubber slider by use of transducers and considering the vertical pressure that is reasonably close to the contact pressure of vehicles, the friction coefficient of the surface is determined. The measurements recorded were then used to establish a method for the harmonization of a majority of the equipment used worldwide.

To normalize the measured data, both a friction measurement and a texture measurement are necessary. Using these values, the friction value at 60km/h [FR(60)] can be calculated. FR(60) values determined using the following equation:

$$FR(60) = DFT_{20} \cdot e^{\frac{-V+20}{Sp}} \qquad [6.6]$$

and

$$Sp = -11.6 + 113.6MTD$$

Where:

FR(60) = Adjusted friction value to 60 km/hr,

DFT_{20} = Friction measured by the DFT at the 20km/h,

V = Slip speed in kilometers per hour,

Sp = Speed constant

Figure 6.13 illustrates a picture of the Dynamic Friction Tester.

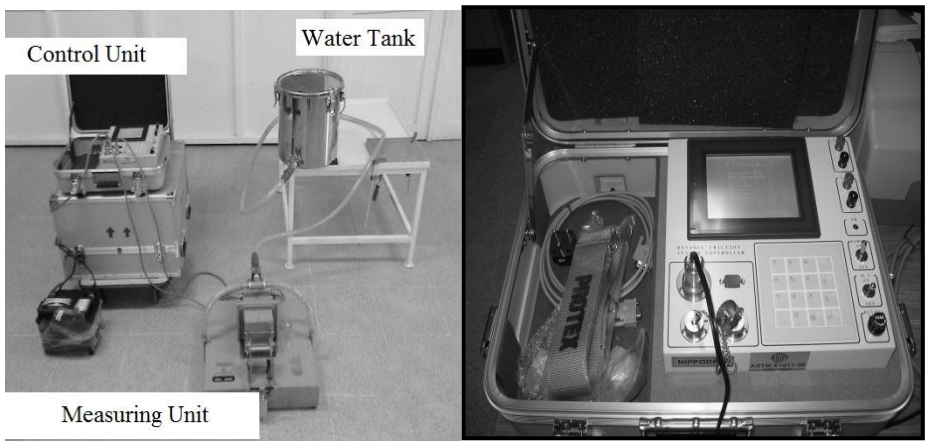

(a) DFT setup (b) DFT control unit

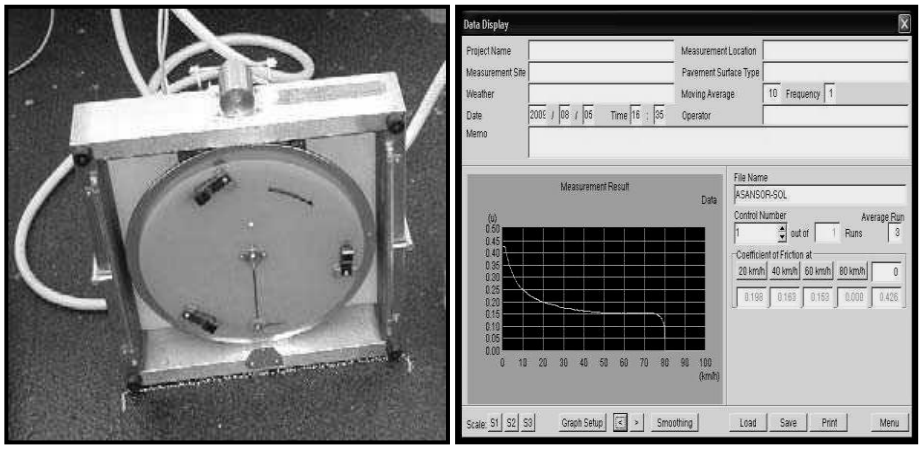

(c) DFT Bottom View (d) data transfer board

Figure 6.13 Dynamic Friction Tester (DFT)

DFT could measure a continuous spectrum of dynamic coefficient of friction of pavement surface over the range of 0 to 80 km/h with good reproducibility (Vollor and Hanson, 2006; Nippou, 2008). In addition, the DFT measurement at 20 km/h is an indication of the microtexture (Hall et al., 2006).

6.6 Results and Discussions

This section contains the results of the different measurements performed on the aggregates and asphalt slabs.

6.6.1 Aggregate Angularity and Flat & Elongated Test Results

Figure 6.17, 6.18 and 6.19 presents the results of the Uncompacted Void Contents and Flow rate of aggregates. Table 6.8 summarizes all the data related to the results of the tests

Based on Figure 6.14, regardless of the aggregate type, the aggregate obtained from Impact crusher have highest flow rate. The flow rate values decreases with the utilization of Roll crusher and Jaw crusher. Flow coefficient values (EN 933-6) for LRA and BRA aggregates more than LJA and BJA for the reason that aggregates crushed with Roll crusher are awfully flaky and because of this reason their flow coefficient values are more than aggregates which crushed with Jaw crusher. As expected, regardless of the crusher type, basalt type aggregate depicted the higher flow rate indicating higher angularity.

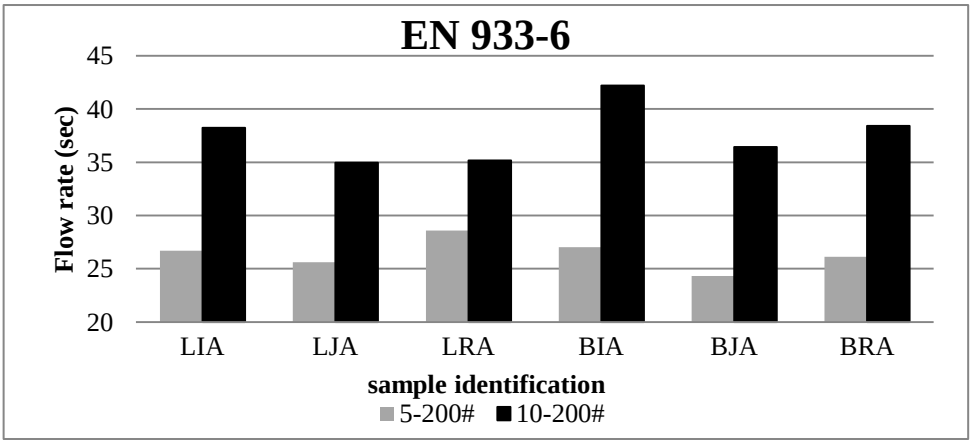

Figure 6.14 Flow Rates of Fine Aggregate Samples by EN 933-6

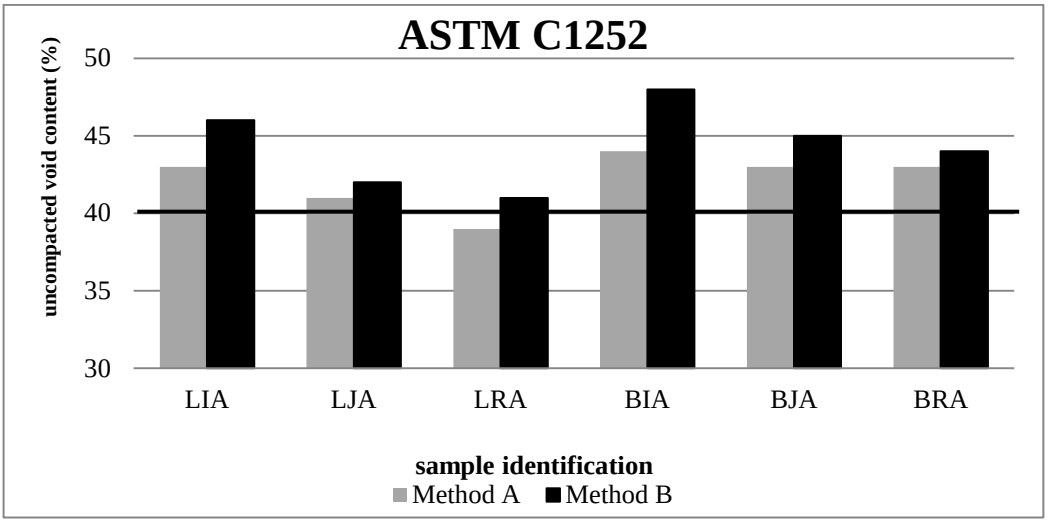

Figure 6.15 uncompacted void contents for fine aggregate (ASTM C1252)

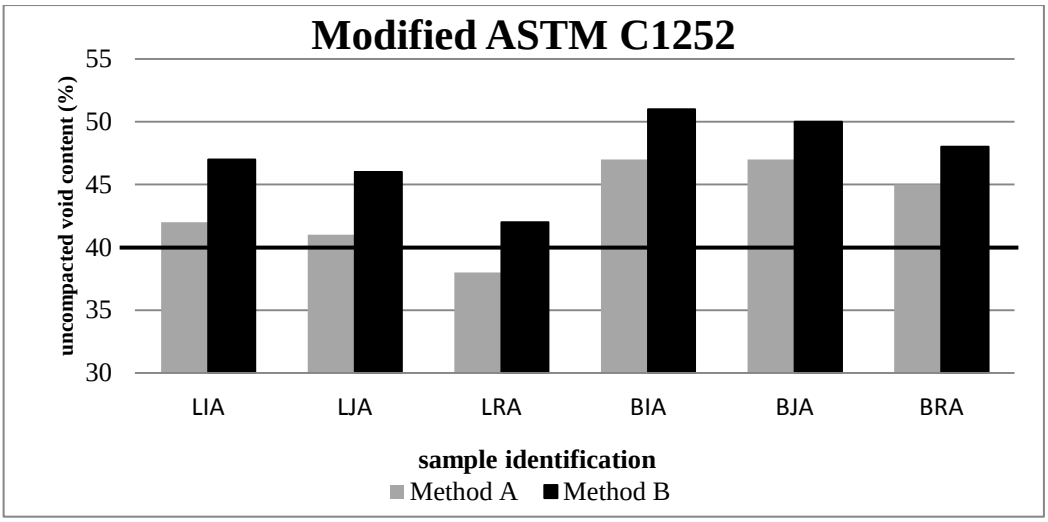

Figure 6.16 uncompacted void contents for coarse aggregate (modified ASTM C1252)

Related to Figure 6.15 and 6.16, basalt type aggregate has higher uncompacted void content in compare with limestone aggregate for all types of crushers. Among the crushers utilized, the Impact crusher displays the higher uncompacted void content, the values decreases with the utilization of Jaw and Roll crusher. It should be mentioned that, the limestone aggregate produced with Roll crushes exceeds the lower limit of uncompacted void content which 40% for both ASTM C1252 and modified ASTM C1252.

Figure 6.17 and 6.18 presents the results of the flat & elongated particles and flakiness index of the samples. Based on the evaluation of the ASTM D4791 and BS 812 results, it can be said that the aggregates prepared with Impact crusher has fewer flat and elongated particles in comparison with the other samples produced with different crusher. Aggregates which crushed with Roll crushers have the highest flat & elongated particle and flaky particle values. Higher flat & elongated particle value is not desirable since the aggregate can be easily broken down during mixing with bitumen and in compaction process.

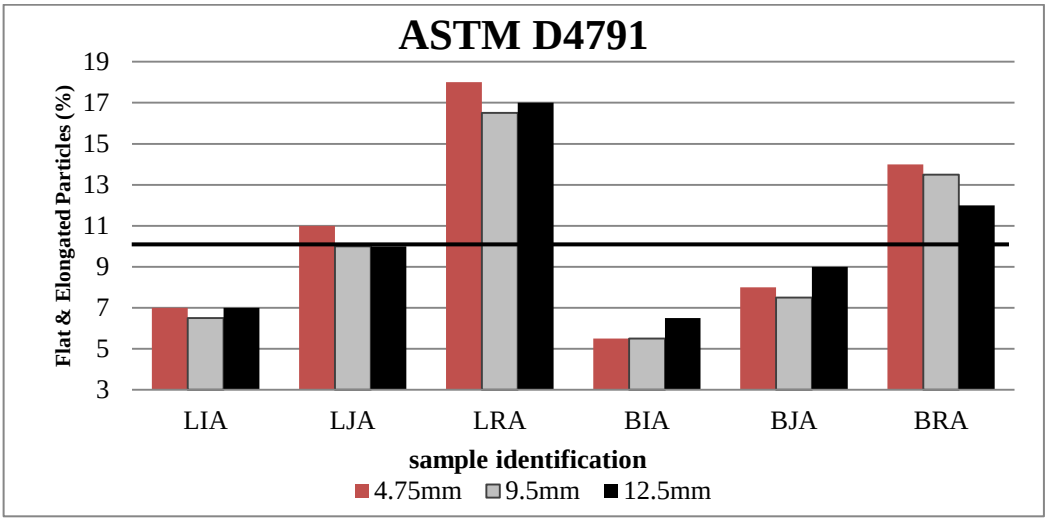

Figure 6.17 Flat and elongated particle results (ASTM D4791)

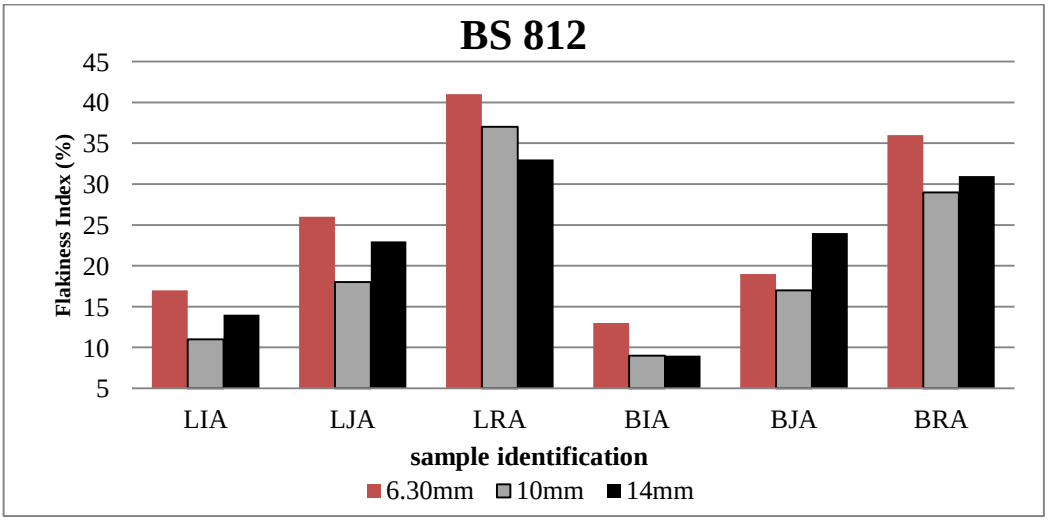

Figure 6.18 Flakiness Index values

Table 6.8 Results of the aggregate angularity and flat & elongated particles.

Aggregate type	Uncompacted Void Content On Standard Graded Sample,% (ASTM C1252)				Flow Coefficient, s (EN 933-6)		Flat & Elongated Particles, (1:3) , % (ASTM D4791)			Flakiness Index, % (BS 812)		
	Fine aggregates		Coarse aggregates									
	Method A	Method B	Method A	Method B	5-200#	10-200#	4.75mm	9.5mm	12.5mm	6.30mm	10mm	14mm
LIA	43	46	42	47	26.71	38.25	7	6.5	7	17	11	14
LJA	41	42	41	46	25.60	34.96	11	10	10	26	18	23
LRA	39	41	38	42	28.58	35.18	18	16.5	17	41	37	33
BIA	44	48	47	51	27.04	42.21	5.5	5.5	6.5	13	9	9
BJA	43	45	47	50	24.32	36.43	8	7.5	9	19	17	24
BRA	43	44	45	48	26.13	38.42	14	13.5	12	36	29	31

6.6.2 Optimum Bitumen Content Determination Results

The data presented in section 6.3 is gained for all hot mix asphalt samples and bitumen content related to 4% air voids is taken as optimum bitumen content. The detailed results are presented in appendix A section. The summarized optimum bitumen contents related to each crusher type and aggregate can be found in Table 6.9.

Table 6.9 optimum bitumen content for each of specimens

Slab name	optimum bitumen content
LIP	4.65
LJP	4.60
LRP	4.60
BIP	4.70
BJP	4.75
MIP	4.70
MJP	4.65
MRP	4.70

6.6.3 Mean Texture Depth and Mean Profile Depth results

The calculated MTD values as well as the MPD values analyzed with MATLAB program can be seen in Figure 6.19.

As depicted in Figure 6.19, among the sample prepared with the same crusher, the sample prepared with basalt aggregate exhibits higher texture and profile depths. Besides, among the samples prepared with the same aggregate type, the samples prepared with roll crusher depicted the lowest surface properties.

The results also indicated that based on basalt and mix type aggregate samples, the aggregate crushed with Impact crusher has the highest MTD and MPD values since the aggregates crushed with Impact crusher have highest angularity.

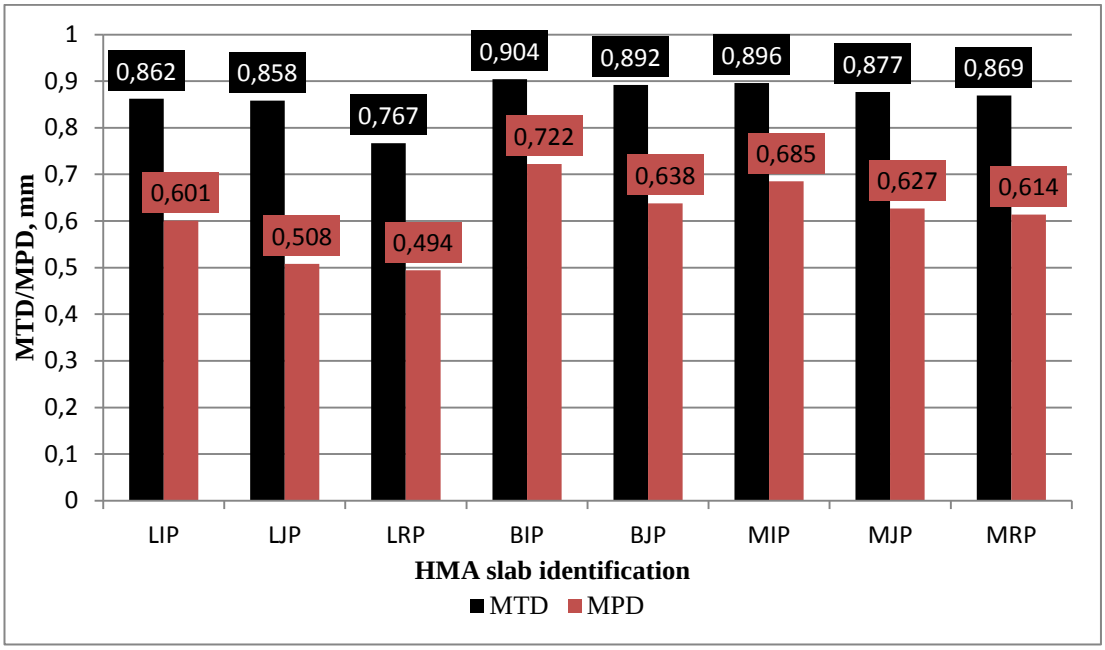

Figure 6.19 MPD and MTD values

6.6.4 Dynamic Friction Test and FR(60) Results

Figure 6.20 presents the measured DFT_{20} values and the calculated FR(60) values.

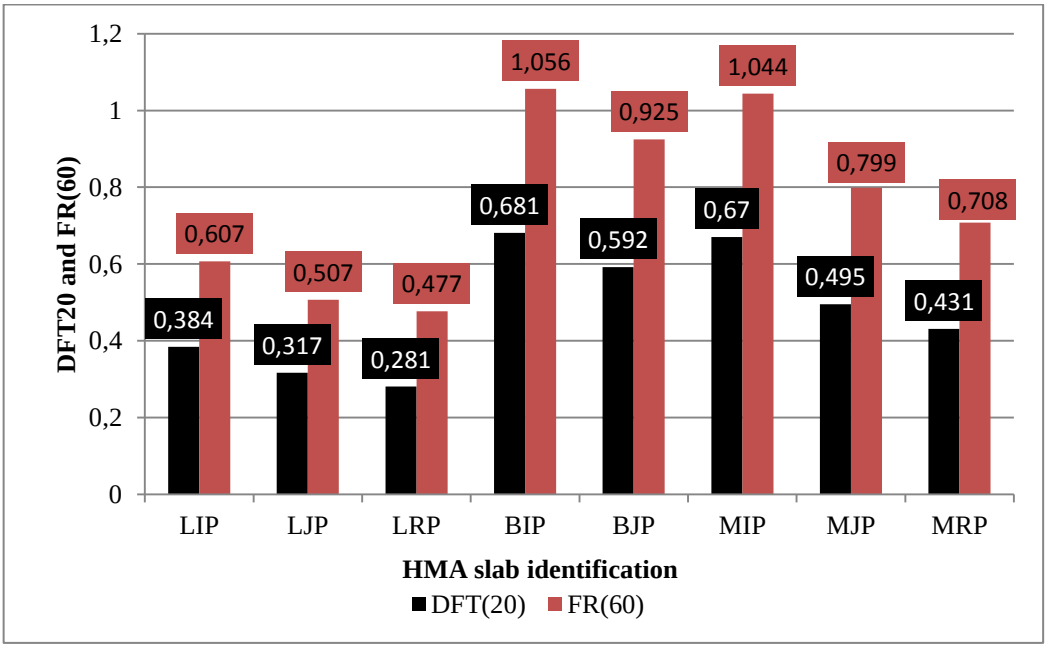

Figure 6.20 Measured Friction Coefficients at 20 km/h and FR(60) values

As seen in Figure 6.20, the sample exhibiting higher texture and profile depth values also depicts higher DFT_{20} and FR(60) values. As expected basalt type aggregates gain higher friction values compared to limestone aggregates crushed with the same type of crusher.

Among the same aggregate type, roll crusher exhibits the lowest, whereas, Impact crushers depicts the highest friction coefficient values.

CHAPTER SEVEN
CONCLUSIONS

One of the most important properties of the pavement is surface texture which contributes to tire-pavement skid resistance. As well as exhibits the close relationship the angularity characteristics of the aggregates used with the flexible pavement.

Based on the results obtained, the following conclusions can be with drawn.

1. EN 933-6 and ASTM C1252 clearly designates the type of aggregate (whether basalt, limestone or mix type) and the type of crusher (whether the aggregate crushed with Impact, Jaw or Roll crusher).

2. Based on the results conducted on the aggregates, basalt type aggregate exhibited higher angularity values compared to limestone aggregate.

3. Among the same type of aggregate, the aggregate crushed with Impact crusher gained the higher angularity values where as Roll crusher exhibited the lowest angularity values.

4. Sand patch and 3D laser scanner are used to evaluate the texture properties of the flexible pavement types involving different aggregate type and crusher. The slab involving basalt type aggregate yielded higher MTD and MPD values in compared to limestone aggregate. The results also indicated that the aggregate crushed with Impact crusher has the highest MTD and MPD values since the aggregates crushed with Impact crusher have higher angularity and more cubical particles in compared with the others.

5. Dynamic friction tester is used to estimate the skid properties of the flexible pavement. The sample exhibiting higher texture and profile depth values also depicts higher DFT_{20} and FR(60) values. As expected basalt type aggregates gain higher friction values compared to limestone aggregates crushed with

the same type of crusher. Also the results depict that the aggregate which crushed with Impact crusher has the higher DFT_{20} and friction value [FR(60)].

REFERENCES

.

AASHTO TP33, (1993). *Standard test method for uncompacted void content of fine aggregate, American Assoc. of State Highway and Transportation Official.* Washington, D.C.

AFNOR P18-564, (1990). *Normalisation Française Determination du Coefficient d'e'coulement des Sables.* PR Industrie, Paris.

Asphalt Institute, (1995). *SUPERPAVE Performance Graded Asphalt Binder.*

Asphalt Institute, (1996). *SUPERPAVE Level 1 Mix Design. Superpave Series No.2 (SP-2).* Lexington, KY.

ASTM C1252, (1998). *Standard test method for uncompacted void content of fine aggregate (as influenced by particle shape, surface texture, and grading). American Society for Testing and Materials*. West Conshohoken, Philadelphia, PA.

ASTM *C136*, (2008). *Standard Method for Sieve Analysis of Fine and Coarse Aggregates.* American Society for Testing and Materials, Printed in Easton, Md., USA.

ASTM D4791-10, (1989). *Standard Test Method for Flat Particles, Elongated Particles, or Flat and Elongated Particles in Coarse Aggregate.* American Society for Testing and Materials, Printed in Easton, Md., USA.

ASTM E 1845-01, (2003). *Standard Practice for Calculating Pavement Macro-Texture Mean Profile Depth*, *04*, 03, ASTM, West Conshohocken, Pennsylvania.

ASTM E 1911-98, (1999). *Standard Test Method for Measuring Pavement Surface Frictional PropertiesUsing the Dynamic Friction Tester*, *04*,03, West Conshohocken, pennsylvania.

ASTM E 965-96, (1998). *Standard Test Method for Measuring Pavement Macro-Texture Depth Using aVolumetric Technique*, *04*, 03, West Conshohocken, Pennsylvania.

ASTM E303-93, (2008). *Standard Test Method for Measuring Surface Frictional Properties Using the British Pendulum Tester.*

Barksdale, R.D. (1991). *The Aggregate Handbook*, National stone association.

Barksdale, R.D. and Itani, S.Y. (1989). *Influence of Aggregate Shape on Base Behavior*, Transportation Research Record 1227, TRB, National Research Council, Washington, D.C., pp. 173-182.

BSI 812: Part 1. *Testing Aggregates. Methods for determination of particle size and shape*, British Standards Institute, 1975.

BSI 812-Part 2. (1995). *Testing aggregates. Methods of determination of density*, British Standards Institute.

Chen, W.F. (1995). *The Civil Engineering Handbook*. CRC Press, Florida.

Collis, L., & Fox, R.A. (1985). *Aggregates: Sand, Gravel and Crushed Rock Aggregates for Construction Purposes*, Engineering Geology Special Publication No:1, The Geological Society of London.

Dahir, S. (1979). *A Review of Aggregate Selection Criteria for Improved Wear Resistance and Skid Resistance of Bituminous Surfaces*. Journal of Testing and Evaluation Vol. 7.

Ergun, M., Iyinam, S., and Iyinam, A. F. (2005) *Prediction of Road Surface Friction Coefficient Using Only Macro and Microtexture Measurements* , Journal. Transportation Engineering, Vol: 131, pp.311–319

Flintsch, G.W., Luo, Y., and Al-Qadi, I.L., (2005). Analysis of the Effect of Pavement Temperature on the Frictional Properties of Flexible Pavement Surfaces. *Presented at 84th Transportation Research Board Annual Meeting*, Washington, D.C.

Freeman, R.B. & Kuo, C-Y., (1999). Quality Control for Natural Sand Content of Asphalt Concrete. *Journal of Transportation Engineering, November/December, ASCE.*

Fulop, I.A., Bogardi, I., Gulyas, A., and Csicsely-Tarpay, M. (2000). Use of Friction and Texture in Pavement Performance Modeling. *ASCE Journal of Transportation Engineering, Vol. 126*, No. 3.

Galloway J. (1994), *Grading, Shape, and Surface Properties* . ASTM Special Technical Publi-cation No. 169C, Philadelphia, pp. 401- 410.

Grieco, F.W. and Grieco, J.P. (1985). *Manufacturing and refurbishing of jaw crushers*, CIM Bull., 78(Oct.), 38.

Gupta, A. (2006) Roll Crushers , Mineral Processing Design and Operation.

Hall, J.W., Glover, L.T., Smith, K.L., Evans, L.D., Wambold, J.C., Yager, T.J., and Rado, Z. (2006). *Guide for Pavement Friction. Project No. 1-43*, Final Guide, National Cooperative Highway Research Program, Transportation Research Board, National Research Council, Washington, D.C.

Hanson, D.I. and Prowell, B.D. (2004). *Evaluation of Circular Texture Meter for Measuring Surface Texture of Pavements*. NCAT Report 04-05, National Center for Asphalt Technology, Auburn, AL.

Henry J.J. (1996). Overview of the International PIARC Experiment to Compare and Harmonize Texture and Skid Resistance Measurements; *The International Friction Index. Proceedings of the 3rd International Symposium on Pavement Surface Characteristics*, Christchurch, New Zealand, September.

Henry, J.J. and Dahir, S. (1979). *Effects of Textures and the Aggregates that produce them on the Performance of Bituminous Surfaces*. Transportation Research Record 712, Transportation Research Board, National Research Council, Washington, D.C.

Hudson B. (1999), *Aggregate Shape Affects Concrete Cost*, Quarry, Noviembre 1998, pp 1-4.

Kowalski, K.J. (2007). *Influence of Mixture Composition on the Noise and Frictional Characteristics of Flexible Pavements.* Ph.D. Dissertation, Purdue University, West Lafayette, IN.

Lewis, F.M., Coburn, J.L., and Bhappu, R.B. (1976). Comminution: *A guide to size-reduction system design.* Min. Engng., 28(Sept.), 29.

Masad, E., B. Muhunthan, N. Shashidhar, and T. Harman, (1999) *Quantifying Laboratory Compaction Effects on the Internal Structure of Asphalt Concrete* Transportation Research Record (TRB), National Research Council, No. 1681, Washington, D.C., pp. 179-185.

Masad, E., D. Olcott, T. White, and L. Tashman, *Correlation of Imaging Shape Indices of Fine Aggregate with Asphalt Mixture Performance,* Presented at the 80th Annual Meeting of the Transportation Research Board, National Research Council.3.

Masad, E., Rezaei, A., Chowdhury, A., and Harris, P. (2009), P*redicting asphalt mixture skid resistance based on aggregate characteristics.*

Masad, E., T. Al-Rousan, J. Button, D. Little, and E. Tutumluer, (2005) *Test Methods for Characterizing Aggregate Shape, Texture and Angularity ,* NCHRP 4-30A Final Report, Report Number 555, National Cooperative Highway Research Program, National Research Council, Washington, D.C.

Mora, C.F., Kwan, A.K. and Chan, H.C. *Particle Size Distribution Analysis of Coarse Aggregate Using Digital Image Processing* , Cement and Concrete Research, Vol 28, No 6, 1998, pp 921.

NCHRP 04-19 (2000) *Validation of Performance-Related Tests of Aggregates for Use in Hot-Mix Asphalt Pavements.*

Neville, A.M. (1997) *Properties of Concrete*. (Third Edition) Longman ltd, England. pp.108-176.

Oduroh, K.P., Mahboub, K.C., & Anderson, R.M. (2000). Flat and Elongated Aggregates in Superpave Regime. *Journal of Materials in Civil Engineering.*

Permanent International Association of Road Congresses (PIARC), (1995) *International PIARC Experiment to Compare and Harmonize Texture and Skid Resistance Measurements* , Report No. AIPCR-01.040.T, PIARC, Brussels, Belgium.

Permanent International Association of Road Congresses (PIARC). (1987) *Report of the Committee on Surface Characteristics* , Proceedings of the 18th World Road Congress, Brussels, Belgium.

Popovics, S. (1979) *Concrete-Making Materials*, McGraw-Hill, U.S.A.

Popovics, S. (1998) *Strength and Related Properties of Concrete* . A Quantitative Approach . John Wiley and Sons.

Powers, T.C., (1966) *The Nature of Concrete , Significance of Tests and Properties of Concrete and Concrete Making Materials*, ASTM Special Technical Publication No. 169A, Philadelphia, , pp. 61-72.

Roberts, F.L., Kandhal, P.S., Brown, E.R., Lee, D.Y., and Kennedy, T.W. (1996). *HMA Materials, Mixture Design, and Construction* . Second Edition, NAPA, Research and Education Foundation.

Saito, K., Horiguchi, T., Kasahara, A., Abe, H., and Henry, J.J. 1996. Development of Portable Tester for Measuring Skid Resistance and Its Speed Dependency on Pavement Surfaces. *Transportation Research Record 1536*, Transportation Research Board, TRB, National Research Council, Washington D.C.

Shupe, J.W. (1960). *Pavement Slipperiness* . Section 20 of the Highway Engineering Handbook by K.B. Woods, McGraw-Hill Book Co., Inc., New York, NY.

Shupe, J.W. and Lounsbury, R.W. (1958). Polishing Characteristics of Mineral Aggregates. *Proceedings First International Skid Prevention Conference,* University of Virginia, Charlottesville, VA.

Topal, A. & Sengoz, B. (2005) *Determination of fine aggregate angularity in relation with the resistance to rutting of hot-mix asphalt* , Construction and Building Materials, March 2005 Issue.

Topal, A. (2001). *Fine aggregate angularity in turkey in bituminous mixtures*. Graduate school of natural and applied sciences of Dokuz Eylul University, Master of science thesis.

Topal, A. (2008). *Agregalarin geometrik özelliklerinin belirlenmesine yönelik yeni görüntü analiz yöntemleri geliştirilmesi.* Graduate school of natural and applied sciences of Dokuz Eylul University, PhD thesis.

Topal, A., & Şengöz, B. (2000). Bitümlü Karışımlarda Kullanılan İnce Taneli Agregaların Köşeliğinin Belirlenmesi ve Kullanılabilirliğinin Saptanması. *3. Ulusal Asfalt Sempozyumu ve Sergisi*,16-17 Kasım, KGM, Ankara, pp.184-194.

U.S. Army Corps of Engineers.(1991). *Hot Mix Asphalt Paving Handbook* .Pub.Un-13. Washington, D.C.

Uluçaylı, M. (1976). The Identification of Failures in Asphaltic Concrete Pavements.

Uluçaylı, M. (1997). Bitümlü Karışımların Tasarımında Yeni Gelişmeler-Yoğurmalı Pres, YTMK, Ankara.

Vollor, T.W. and Hanson, D.I. (2006). Development of Laboratory Procedure for Measuring Friction of HMA Mixtures-Phase 1. *NCAT Report 06-06*, National Center of Asphalt Technology, Auburn University, AL.

Wallman, C.G. and Astron, H. (2001). Friction Measurement Methods and the Correlation between Road Friction and Traffic Safety. Swedish National Road and Transport Research Institute, *VTI Meddelande 911A*, Linköping, Sweden. Washington, D.C.

Wills, B.A. (1984). Mineral Processing Technology (2nd Edition). NewYork.

APPENDIX A
MIXTURE DESIGN

Table A-1 Marshall mix design for LIP sample

Specimen No.	Bitumen %		Specimen Height (mm)				Weight in air (gr.)	Weight in water (gr.)	SSD weight (gr.)	Volume	Bulk specific gravity	Max. teo. specific gravity	Voids (%)	VMA	VFA	Flow (mm)	Stability (kgf)	Correlation fact.	Corr. Stability (kgf)
	Wa	Wb	1	2	3	Avg.	A	C	B	V	Dp	Dt	Vh	%	%	mm	kgf		kgf
1	4.0	3.8	62.32	62.24	62.28	62.3	1186.3	693.1	1196.4	503.3	2.357	2.5302	6.844	14.83	53.9	1.74	1088	1.030	1121
2	4.0	3.8	60.72	60.94	60.82	60.8	1182.4	692.6	1189.1	496.5	2.381	2.5302	5.878	13.95	57.9	1.67	1139	1.074	1223
3	4.0	3.8	61.42	61.28	61.36	61.4	1189.2	696.7	1197.1	500.4	2.376	2.5302	6.075	14.13	57.0	1.66	1150	1.056	1214
Avg.											2.372		6.265	14.30	56.2	1.69			1186
1	4.5	4.3	60.92	60.82	60.98	60.9	1197.2	701.2	1199.3	498.1	2.404	2.5127	4.343	13.57	68.0	2.00	1157	1.071	1239
2	4.5	4.3	60.92	60.68	60.74	60.8	1191.6	700.3	1198.3	498.0	2.393	2.5127	4.771	13.95	65.8	1.78	1148	1.074	1233
3	4.5	4.3	61.02	61.48	61.14	61.2	1204.2	704.3	1209.1	504.8	2.385	2.5127	5.061	14.21	64.4	1.99	1089	1.062	1157
Avg.											2.394		4.725	13.91	66.1	1.92			1210
1	5.0	4.8	60.76	60.98	60.82	60.9	1198.3	710.1	1205.3	495.2	2.420	2.4955	3.033	13.39	77.4	2.88	1108	1.071	1187
2	5.0	4.8	60.92	61.08	60.88	61.0	1198.0	710.3	1204.3	494.0	2.425	2.4955	2.822	13.20	78.6	2.28	1040	1.068	1111
3	5.0	4.8	60.72	60.88	60.94	60.8	1198.9	711.3	1204.4	493.1	2.431	2.4955	2.572	12.98	80.2	2.56	1098	1.074	1179
Avg.											2.425		2.809	13.19	78.7	2.57			1159
1	5.5	5.2	61.58	61.72	61.42	61.6	1210.4	716.4	1214.1	497.7	2.432	2.4788	1.888	13.37	85.9	3.81	1074	1.049	1127
2	5.5	5.2	61.44	61.32	61.48	61.4	1202.4	711.3	1207.3	496.0	2.424	2.4788	2.202	13.65	83.9	3.05	978	1.056	1033
3	5.5	5.2	60.88	61.10	60.96	61.0	1198.8	708.9	1206.2	497.3	2.411	2.4788	2.750	14.13	80.5	2.52	959	1.068	1024
Avg.											2.422		2.280	13.72	83.4	3.13			1061

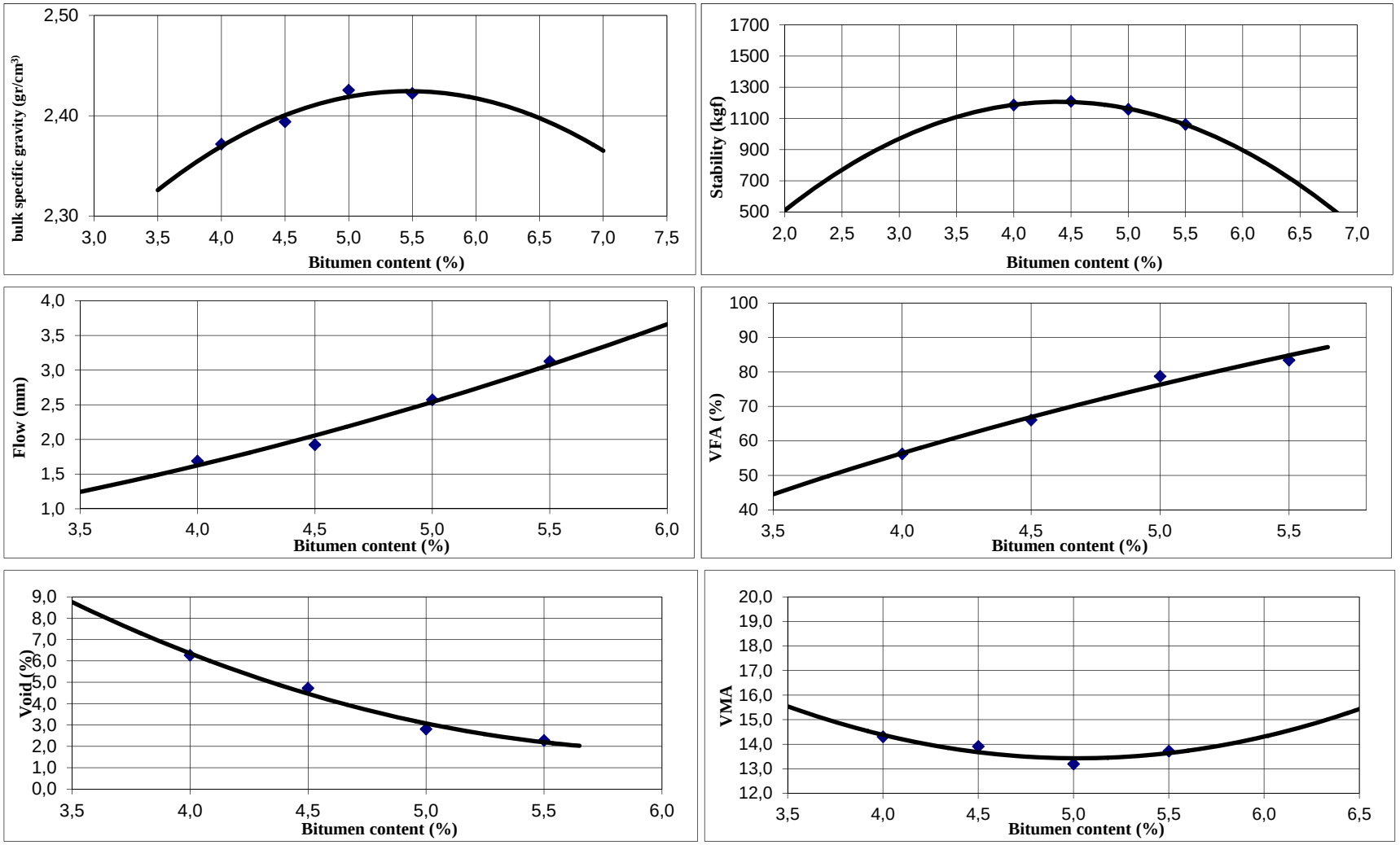

Figure A-1 Marshall mix design graphics for LIP sample

Table A-2 Marshall mix design for LJP sample

Specimen No.	Bitumen %		Specimen Height (mm)				Weight in air (gr.)	Weight in water (gr.)	SSD weight (gr.)	Volume	Bulk specific gravity	Max. teo. specific gravity	Voids (%)	VMA	VFA	Flow (mm)	Stability (kgf)	Correlation fact.	Corr. Stability (kgf)
	Wa	Wb	1	2	3	Avg.	A	C	B	V	Dp	Dt	Vh	%	%	mm	kgf		kgf
1	4.0	3.8	59.96	60.24	60.12	60.1	1164.2	681.3	1171.2	489.9	2.376	2.5302	6.078	14.13	57.0	2.08	1099	1.096	1205
2	4.0	3.8	61.78	61.24	61.58	61.5	1186.9	692.9	1191.8	498.9	2.379	2.5302	5.974	14.03	57.4	2.12	1056	1.053	1112
3	4.0	3.8	61.10	60.92	60.88	61.0	1192.9	691.1	1196.8	505.7	2.359	2.5302	6.770	14.76	54.1	2.10	985	1.068	1052
Avg.											2.371		6.274	14.31	56.2	2.10			1123
1	4.5	4.3	61.10	61.34	61.08	61.2	1196.2	693.3	1199.7	506.4	2.362	2.5127	5.989	15.05	60.2	2.32	1119	1.062	1188
2	4.5	4.3	61.04	61.18	61.30	61.2	1187.9	692.8	1192.3	499.5	2.378	2.5127	5.352	14.48	63.0	2.27	1203	1.062	1278
3	4.5	4.3	60.42	60.52	60.84	60.6	1195.7	701.8	1197.1	495.3	2.414	2.5127	3.923	13.19	70.2	1.90	1058	1.081	1144
Avg.											2.385		5.088	14.24	64.5	2.16			1203
1	5.0	4.8	61.12	61.18	61.08	61.1	1195.9	705.7	1197.6	491.9	2.431	2.4955	2.578	12.99	80.1	2.60	1071	1.065	1141
2	5.0	4.8	61.06	61.28	61.18	61.2	1202.8	711.7	1204.4	492.7	2.441	2.4955	2.175	12.63	82.8	3.33	1050	1.062	1115
3	5.0	4.8	60.56	61.00	60.68	60.7	1200.7	711.1	1201.6	490.5	2.448	2.4955	1.908	12.39	84.6	2.26	1022	1.078	1102
Avg.											2.440		2.220	12.67	82.5	2.73			1119
1	5.5	5.2	61.32	61.30	61.26	61.3	1206.2	711.9	1207.1	495.2	2.436	2.4788	1.735	13.24	86.9	3.01	987	1.059	1045
2	5.5	5.2	61.22	61.18	61.32	61.2	1206.3	708.9	1207.8	498.9	2.418	2.4788	2.455	13.87	82.3	3.29	986	1.062	1047
3	5.5	5.2	60.94	61.20	61.28	61.1	1200.8	707.8	1201.9	494.1	2.430	2.4788	1.957	13.43	85.4	3.18	920	1.065	980
Avg.											2.428		2.049	13.51	84.9	3.16			1024

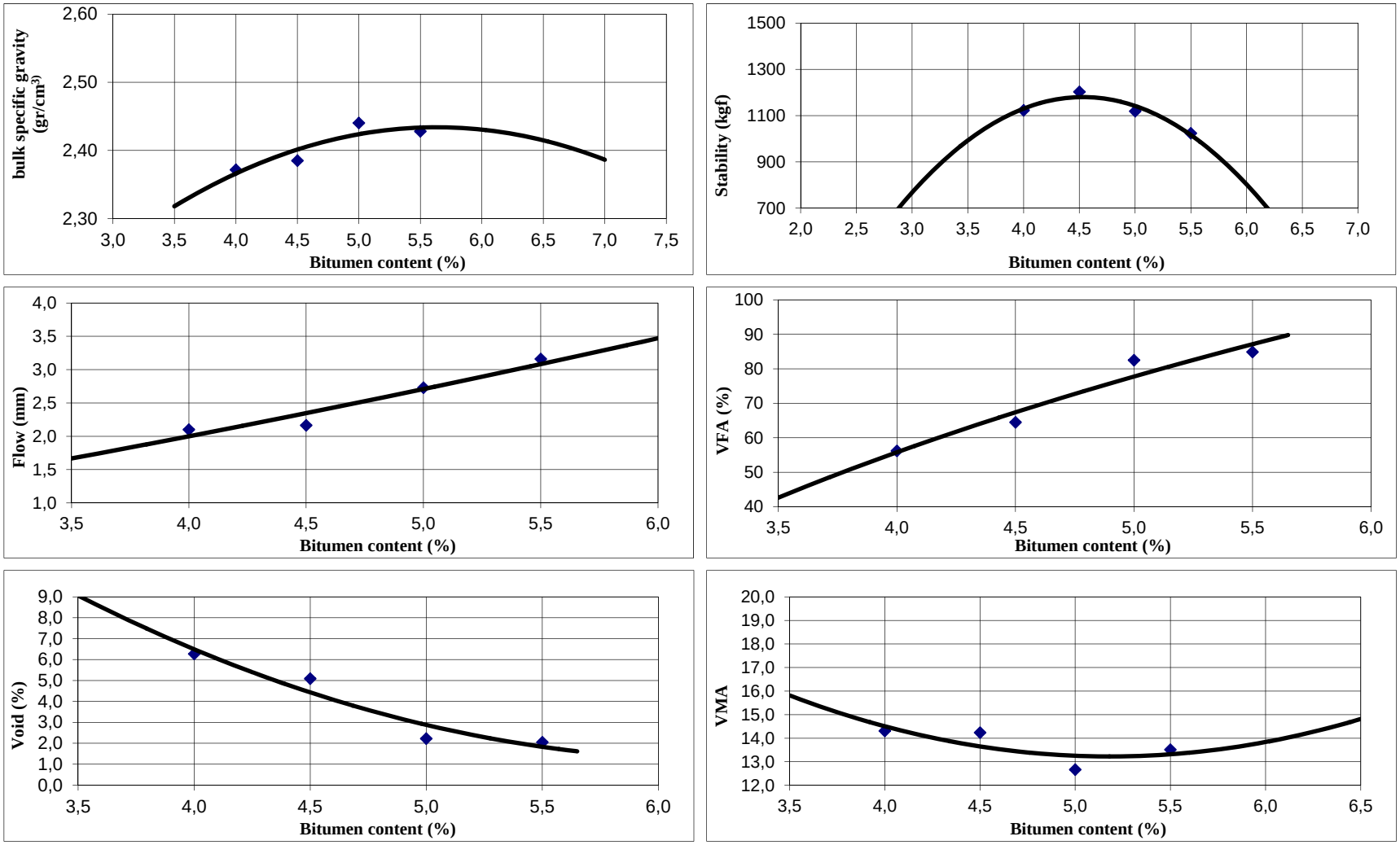

Figure A-2 Marshall mix design graphics for LJP sample

Table A-3 Marshall mix design for LRP sample

Specimen No.	Bitumen %		Specimen Height (mm)				Weight in air (gr.)	Weight in water (gr.)	SSD weight (gr.)	Volume	Bulk specific gravity	Max. teo. specific gravity	Voids (%)	VMA	VFA	Flow (mm)	Stability (kgf)	Correlation fact.	Corr. Stability (kgf)
	Wa	Wb	1	2	3	Avg.	A	C	B	V	Dp	Dt	Vh	%	%	mm	kgf		kgf
1	4.0	3.8	61.78	61.70	61.58	61.7	1185.7	681.1	1193.0	511.9	2.316	2.5097	7.708	16.30	52.7	2.08	1101	1.046	1047
2	4.0	3.8	61.20	61.38	61.36	61.3	1190.1	693.2	1193.8	500.6	2.377	2.5097	5.274	14.10	62.6	1.73	1181	1.059	1145
3	4.0	3.8	61.42	61.48	61.32	61.4	1183.8	692.4	1188.3	495.9	2.387	2.5097	4.883	13.74	64.5	1.92	1205	1.056	1167
Avg.											2.360		5.955	14.71	59.9	1.91			1120
1	4.5	4.3	61.58	61.64	61.52	61.6	1188.6	688.1	1192.3	504.2	2.357	2.4926	5.423	15.22	64.4	2.20	1162	1.049	1114
2	4.5	4.3	60.78	60.56	60.62	60.7	1192.7	693.6	1194.1	500.5	2.383	2.4926	4.395	14.30	69.3	2.39	1436	1.078	1225
3	4.5	4.3	60.20	60.28	60.40	60.3	1188.1	697.6	1190.1	492.5	2.412	2.4926	3.216	13.25	75.7	2.27	1514	1.090	1214
Avg.											2.384		4.345	14.26	69.8	2.29			1184
1	5.0	4.8	60.52	60.36	60.48	60.5	1194.6	694.8	1195.5	500.7	2.386	2.4758	3.632	14.61	75.1	2.63	1150	1.084	1247
2	5.0	4.8	60.44	61.00	60.78	60.7	1198.5	700.5	1199.4	498.9	2.402	2.4758	2.969	14.02	78.8	3.33	1244	1.078	1179
3	5.0	4.8	60.42	60.28	60.36	60.4	1195.3	700.3	1196.5	496.2	2.409	2.4758	2.701	13.78	80.4	2.65	1254	1.087	1177
Avg.											2.399		3.101	14.14	78.1	2.87			1201
1	5.5	5.2	61.40	61.18	61.28	61.3	1207.1	700.4	1208.1	507.7	2.378	2.4594	3.327	15.31	78.3	3.40	1027	1.059	1088
2	5.5	5.2	61.00	60.88	61.22	61.0	1198.0	690.8	1198.4	507.6	2.360	2.4594	4.037	15.93	74.7	3.42	1012	1.068	1081
3	5.5	5.2	60.92	60.54	60.80	60.8	1194.2	698.3	1194.8	496.5	2.405	2.4594	2.202	14.32	84.6	3.84	1049	1.074	1127
Avg.											2.381		3.189	15.19	79.2	3.55			1098

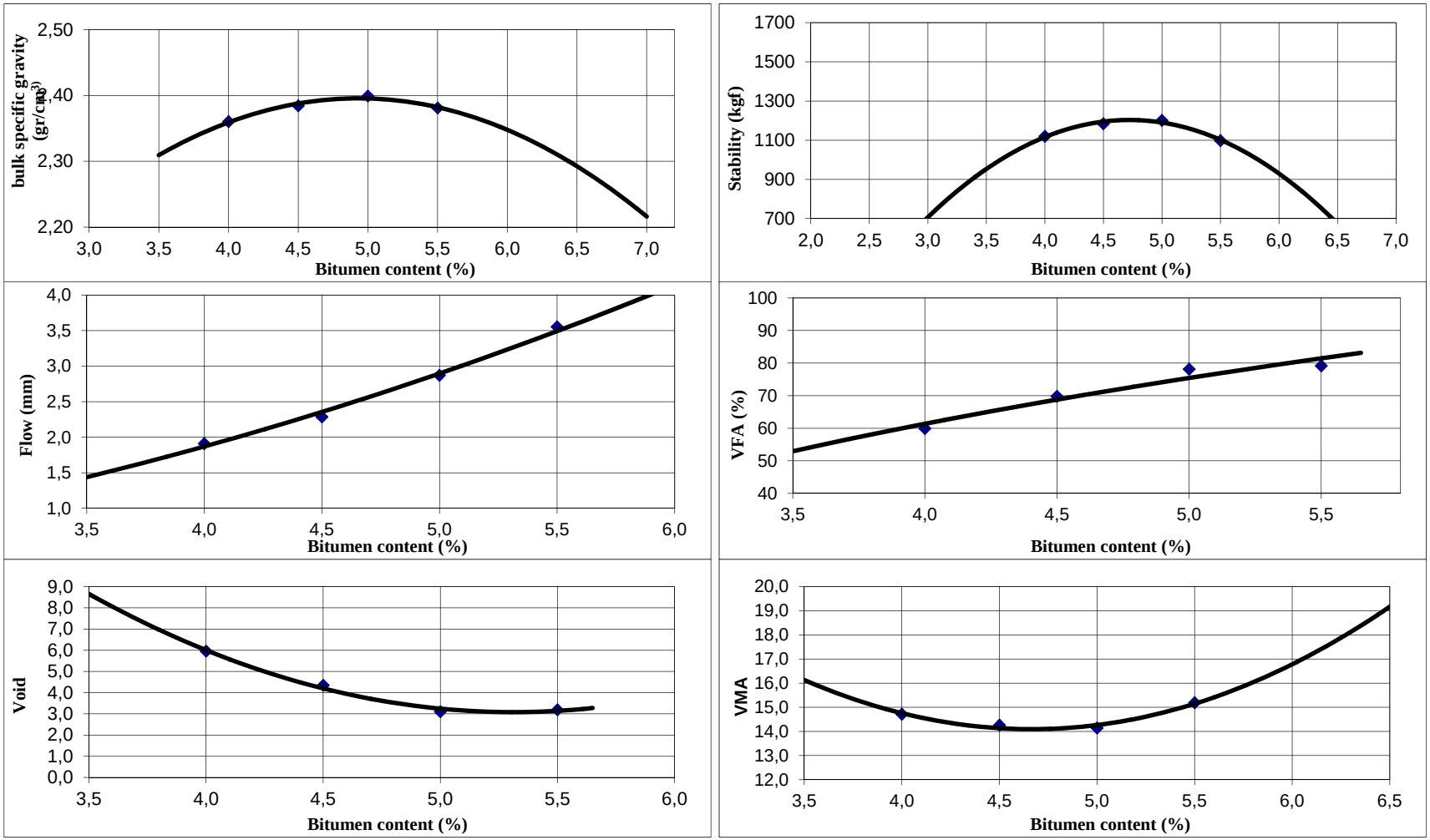

Figure A-3Marshall mix design graphics for LRP sample

Table A-4 Marshall mix design for BIP sample

Specimen No.	Bitumen %		Specimen Height (mm)				Weight in air (gr.)	Weight in water (gr.)	SSD weight (gr.)	Volume	Bulk specific gravity	Max. teo. specific gravity	Voids (%)	VMA	VFA	Flow (mm)	Stability (kgf)	Correlation fact.	Corr. Stability (kgf)
	Wa	Wb	1	2	3	Avg.	A	C	B	V	Dp	Dt	Vh	%	%	mm	kgf		kgf
1	4.0	3.8	65.34	65.18	65.66	65.4	1195.0	679.6	1196.5	516.9	2.312	2.4644	6.189	13.84	55.3	2.09	1172	0.954	1118
2	4.0	3.8	65.42	65.40	65.68	65.5	1178.1	672.1	1186.4	514.3	2.291	2.4644	7.05	14.63	51.8	2.65	1021	0.953	973
3	4.0	3.8	64.96	64.92	65.12	65.0	1187.2	675.3	1195.5	520.2	2.282	2.4644	7.392	14.94	50.5	1.91	1073	0.963	1033
Avg.											2.295		6.876	14.47	52.5	2.22			1041
1	4.5	4.3	64.74	64.62	64.98	64.8	1182.9	676.3	1193.7	517.4	2.286	2.4480	6.609	15.20	56.5	2.42	1255	0.968	1215
2	4.5	4.3	64.28	64.36	64.52	64.4	1191.2	682.1	1192.0	509.9	2.336	2.4480	4.571	13.35	65.8	2.13	1332	0.978	1303
3	4.5	4.3	64.52	64.26	64.92	64.6	1195.2	684.9	1196.9	512.0	2.334	2.4480	4.643	13.42	65.4	2.17	1314	0.973	1279
Avg.											2.319		5.274	13.99	62.6	2.24			1265
1	5.0	4.8	63.98	63.42	63.38	63.6	1202.4	685.4	1193.8	508.4	2.365	2.4321	2.755	12.70	78.3	2.75	1308	0.998	1305
2	5.0	4.8	63.84	63.52	63.94	63.8	1204.7	688.6	1200.9	512.3	2.352	2.4321	3.310	13.19	74.9	2.44	1459	0.993	1449
3	5.0	4.8	64.14	63.96	64.00	64.0	1197.6	686.9	1191.1	504.2	2.375	2.4321	2.336	12.32	81.0	2.59	1348	0.988	1332
Avg.											2.364		2.800	12.74	78.1	2.59			1362
1	5.5	5.2	64.26	63.68	63.92	64.0	1200.4	691.3	1201.6	510.3	2.352	2.4164	2.653	13.58	80.5	2.21	1214	0.988	1199
2	5.5	5.2	63.18	63.42	63.84	63.5	1195.3	685.3	1197.1	511.8	2.335	2.4164	3.350	14.20	76.4	3.09	1227	1.000	1227
3	5.5	5.2	64.56	64.94	62.42	64.0	1198.2	688.5	1190.2	501.7	2.388	2.4164	1.166	12.26	90.5	3.46	1243	0.988	1228
Avg.											2.359		2.390	13.34	82.5	2.92			1218

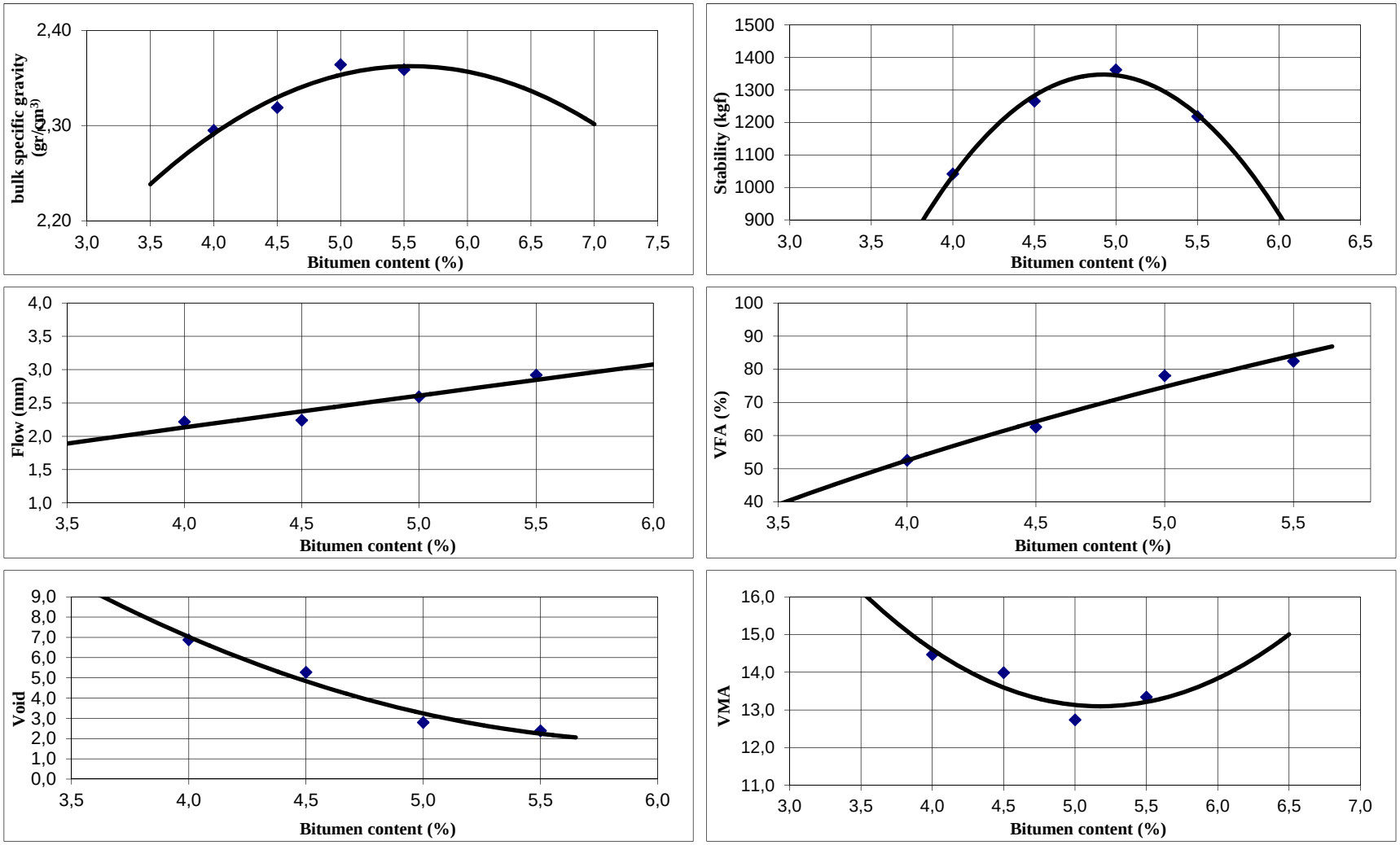

Figure A-4 Marshall mix design graphics for BIP sample

Table A-5 Marshall mix design for BJP sample

Specimen No.	Bitumen %		Specimen Height (mm)				Weight in air (gr.)	Weight in water (gr.)	SSD weight (gr.)	Volume	Bulk specific gravity	Max. teo. specific gravity	Voids (%)	VMA	VFA	Flow (mm)	Stability (kgf)	Correlation fact.	Corr. Stability (kgf)
	Wa	Wb	1	2	3	Avg.	A	C	B	V	Dp	Dt	Vh	%	%	mm	kgf		kgf
1	4.0	3.8	64.28	64.80	64.34	64.5	1179.0	672.1	1196.5	524.4	2.248	2.4386	7.805	15.55	49.8	1.84	1056	0.975	1030
2	4.0	3.8	63.86	64.12	63.80	63.9	1168.1	669.2	1186.4	517.2	2.259	2.4386	7.39	15.17	51.3	2.23	1078	0.990	1067
3	4.0	3.8	64.12	64.52	64.20	64.3	1175.4	670.7	1195.5	524.8	2.240	2.4386	8.157	15.88	48.6	2.12	943	0.980	924
Avg.											2.249		7.783	15.53	49.9	2.06			1007
1	4.5	4.3	63.18	63.22	63.46	63.3	1183.4	679.8	1194.7	514.9	2.298	2.4227	5.136	14.09	63.5	2.44	1195	1.005	1201
2	4.5	4.3	64.02	64.28	63.94	64.1	1189.2	683.7	1193.0	509.3	2.335	2.4227	3.623	12.72	71.5	2.52	1238	0.985	1219
3	4.5	4.3	64.34	64.26	63.86	64.2	1179.9	678.4	1197.9	519.5	2.271	2.4227	6.254	15.10	58.6	2.27	1273	0.983	1251
Avg.											2.302		5.004	13.97	64.5	2.41			1224
1	5.0	4.8	63.88	63.64	63.40	63.6	1193.6	683.4	1195.8	512.4	2.329	2.4072	3.232	13.34	75.8	2.14	1347	0.998	1344
2	5.0	4.8	62.26	62.70	62.94	62.6	1195.4	685.7	1202.9	517.2	2.311	2.4072	3.985	14.01	71.6	2.76	1295	1.023	1325
3	5.0	4.8	63.94	64.08	64.00	64.0	1199.6	686.2	1194.1	507.9	2.362	2.4072	1.883	12.13	84.5	2.62	1306	1.01	1319
Avg.											2.334		3.033	13.16	77.3	2.51			1329
1	5.5	5.2	63.64	63.68	63.22	63.5	1204.1	694.3	1199.6	505.3	2.383	2.3920	0.380	11.77	96.8	2.90	1247	1.000	1247
2	5.5	5.2	63.08	62.92	62.86	63.0	1198.7	691.0	1193.1	502.1	2.387	2.3920	0.195	11.60	98.3	2.74	1304	1.013	1321
3	5.5	5.2	62.68	62.74	63.22	62.9	1197.6	690.5	1204.3	513.8	2.331	2.3920	2.557	13.70	81.3	3.58	1258	1.015	1277
Avg.											2.367		1.044	12.36	92.1	3.07			1282

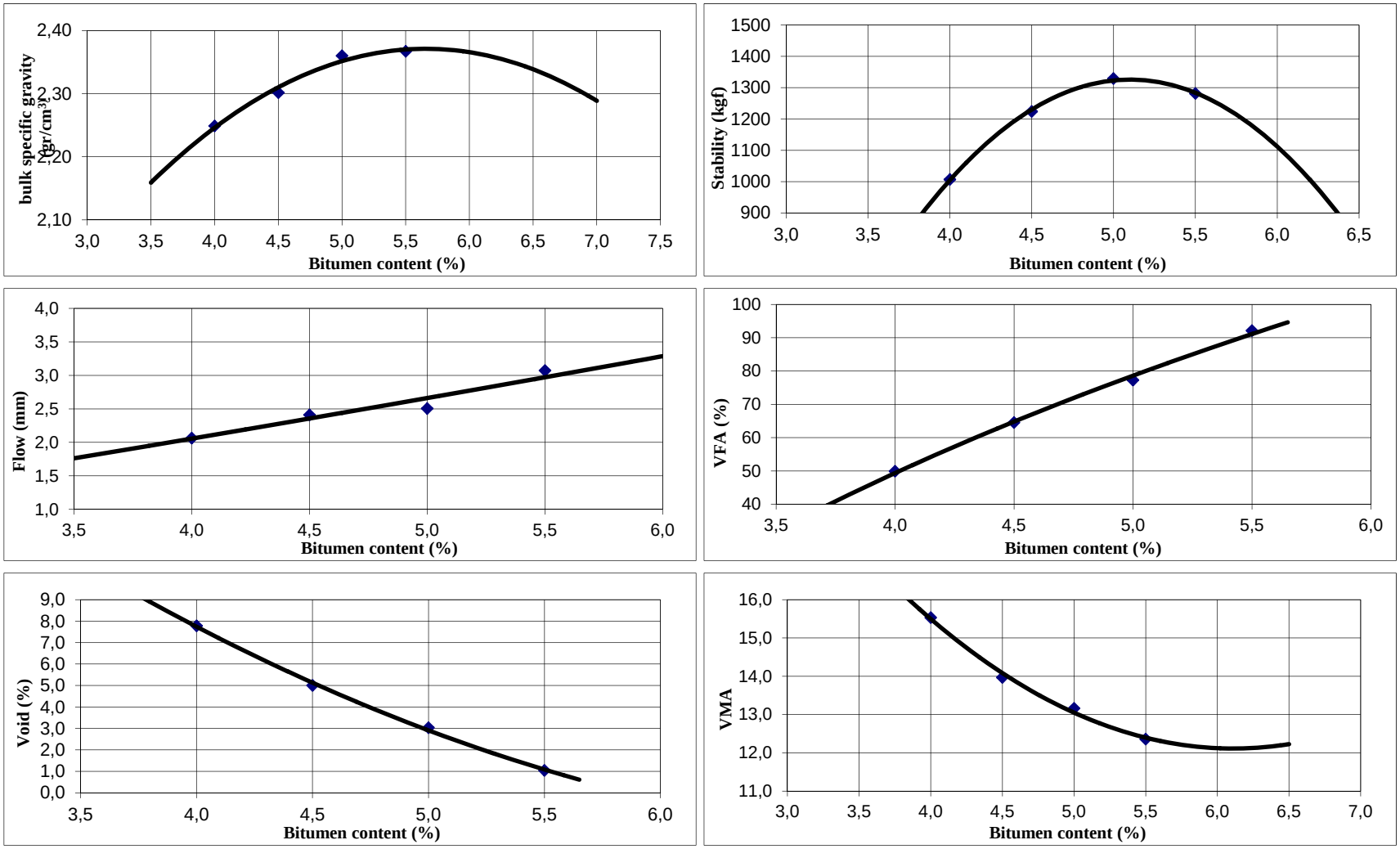

Figure A-5 Marshall mix design graphics for BJP sample

Table A-6 Marshall mix design for MIP sample

Specimen No.	Bitumen %		Specimen Height (mm)				Weight in air (gr.)	Weight in water (gr.)	SSD weight (gr.)	Volume	Bulk specific gravity	Max. teo. specific gravity	Voids (%)	VMA	VFA	Flow (mm)	Stability (kgf)	Correlation fact.	Corr. Stability (kgf)
	Wa	Wb	1	2	3	Avg.	A	C	B	V	Dp	Dt	Vh	%	%	mm	kgf		kgf
1	4.0	3.8	66.74	66.86	67.00	66.9	1180.0	662.0	1192.0	530.0	2.226	2.3697	6.047	16.38	63.1	2.02	1240	0.925	1147
2	4.0	3.8	66.62	66.34	65.82	66.3	1177.0	663.5	1189.5	526.0	2.238	2.3697	5.57	15.95	65.1	2.77	1287	0.938	1207
3	4.0	3.8	65.16	65.28	65.52	65.3	1176.0	664.5	1188.5	524.0	2.244	2.3697	5.293	15.70	66.3	1.85	1246	0.956	1191
Avg.											2.236		5.638	16.01	64.8	2.21			1182
1	4.5	4.3	66.26	66.00	66.18	66.1	1183.5	662.0	1191.0	529.0	2.237	2.3550	5.001	16.37	69.4	2.69	1392	0.941	1310
2	4.5	4.3	65.00	65.06	65.20	65.1	1180.5	665.0	1189.5	524.5	2.251	2.3550	4.429	15.87	72.1	2.18	1374	0.960	1319
3	4.5	4.3	66.00	65.64	65.90	65.8	1181.5	663.0	1189.0	526.0	2.246	2.3550	4.621	16.04	71.2	2.14	1380	0.947	1307
Avg.											2.245		4.684	16.09	70.9	2.34			1312
1	5.0	4.8	65.62	66.00	65.60	65.7	1189.5	678.0	1207.5	529.5	2.246	2.3407	4.025	16.43	75.5	2.08	1329	0.949	1261
2	5.0	4.8	65.70	65.72	65.70	65.7	1198.0	679.5	1213.5	534.0	2.243	2.3407	4.153	16.54	74.9	2.31	1354	0.949	1285
3	5.0	4.8	64.64	64.78	64.62	64.7	1183.5	672.0	1198.5	526.5	2.248	2.3407	3.965	16.37	75.8	2.06	1394	0.970	1352
Avg.											2.246		4.048	16.45	75.4	2.15			1299
1	5.5	5.2	64.14	64.44	64.42	64.3	1200.0	688.5	1224.5	536.0	2.239	2.3266	3.774	17.11	77.9	2.14	1219	0.980	1195
2	5.5	5.2	65.00	65.00	65.28	65.1	1200.0	681.5	1218.0	536.5	2.237	2.3266	3.863	17.18	77.5	2.65	1172	0.960	1125
3	5.5	5.2	64.66	64.30	64.52	64.5	1196.0	682.5	1217.5	535.0	2.236	2.3266	3.915	17.23	77.3	3.46	1177	0.975	1148
Avg.											2.237		3.851	17.17	77.6	2.75			1156

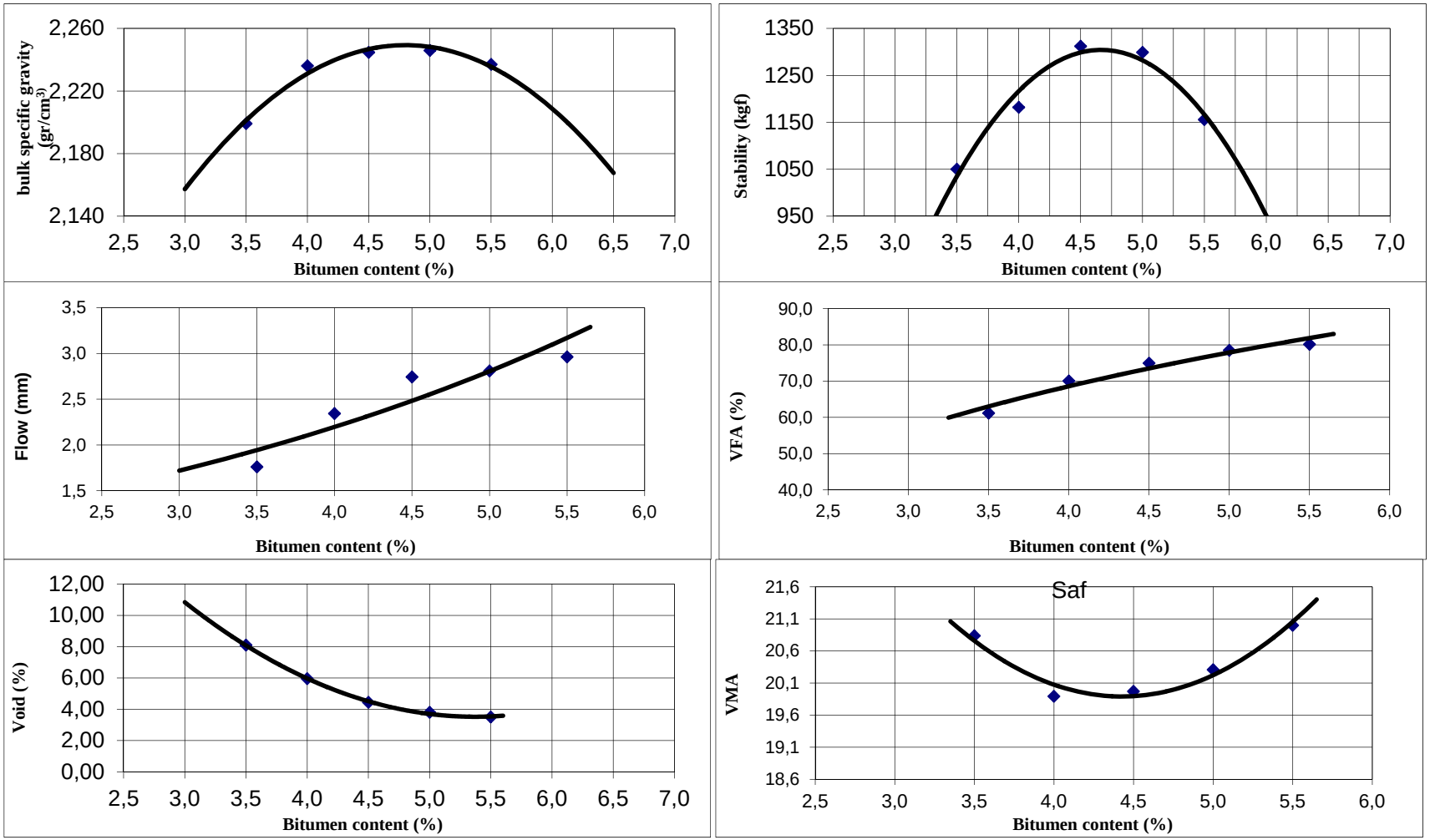

Figure A-6 Marshall mix design graphics for MIP sample

Table A-7 Marshall mix design for MJP sample

Specimen No.	Bitumen %		Specimen Height (mm)				Weight in air (gr.)	Weight in water (gr.)	SSD weight (gr.)	Volume	Bulk specific gravity	Max. teo. specific gravity	Voids (%)	VMA	VFA	Flow (mm)	Stability (kgf)	Correlation fact.	Corr. Stability (kgf)
	Wa	Wb	1	2	3	Avg.	A	C	B	V	Dp	Dt	Vh	%	%	mm	kgf		kgf
1	4.0	3.8	64.32	64.54	64.58	64.5	1189.0	680.5	1196.5	516.0	2.304	2.4558	6.170	13.45	54.1	2.02	1377	0.975	1343
2	4.0	3.8	64.52	64.40	64.68	64.5	1171.1	668.4	1186.4	518.0	2.261	2.4558	7.94	15.08	47.4	2.77	873	0.975	851
3	4.0	3.8	64.62	64.90	65.08	64.9	1182.9	677.4	1195.5	518.1	2.283	2.4558	7.030	14.24	50.6	1.85	973	0.965	939
Avg.											2.283		7.047	14.26	50.7	2.21			1044
1	4.5	4.3	63.74	64.02	63.98	63.9	1186.5	681.8	1193.7	511.9	2.318	2.4396	4.992	13.36	62.6	2.69	1170	0.990	1158
2	4.5	4.3	63.42	63.36	63.48	63.4	1187.9	683.2	1192.0	508.8	2.335	2.4396	4.300	12.73	66.2	2.18	1232	1.003	1236
3	4.5	4.3	64.32	64.26	64.58	64.4	1192.1	682.2	1196.9	514.7	2.316	2.4396	5.062	13.42	62.3	2.14	1217	0.978	1190
Avg.											2.323		4.785	13.17	63.7	2.34			1195
1	5.0	4.8	63.32	63.20	63.38	63.3	1192.4	690.3	1195.8	505.5	2.359	2.4238	2.679	12.25	78.1	2.08	1211	1.005	1217
2	5.0	4.8	63.08	63.52	64.34	63.6	1199.7	692.8	1202.9	510.1	2.352	2.4238	2.966	12.50	76.3	2.31	1364	0.998	1361
3	5.0	4.8	63.30	62.96	63.00	63.1	1191.8	687.9	1194.1	506.2	2.354	2.4238	2.863	12.41	76.9	2.06	1235	1.01	1247
Avg.											2.355		2.836	12.39	77.1	2.15			1275
1	5.5	5.2	63.62	63.68	63.22	63.5	1181.9	694.3	1199.6	505.3	2.339	2.4083	2.878	13.40	78.5	2.14	1104	1.000	1104
2	5.5	5.2	62.78	62.42	62.84	62.7	1181.5	692.3	1193.1	500.8	2.359	2.4083	2.038	12.65	83.9	2.65	1136	1.020	1159
3	5.5	5.2	62.68	61.94	62.12	62.2	1180.5	691.5	1188.2	496.7	2.377	2.4083	1.313	12.00	89.1	3.46	1169	1.033	1208
Avg.											2.358		2.077	12.68	83.8	2.75			1157

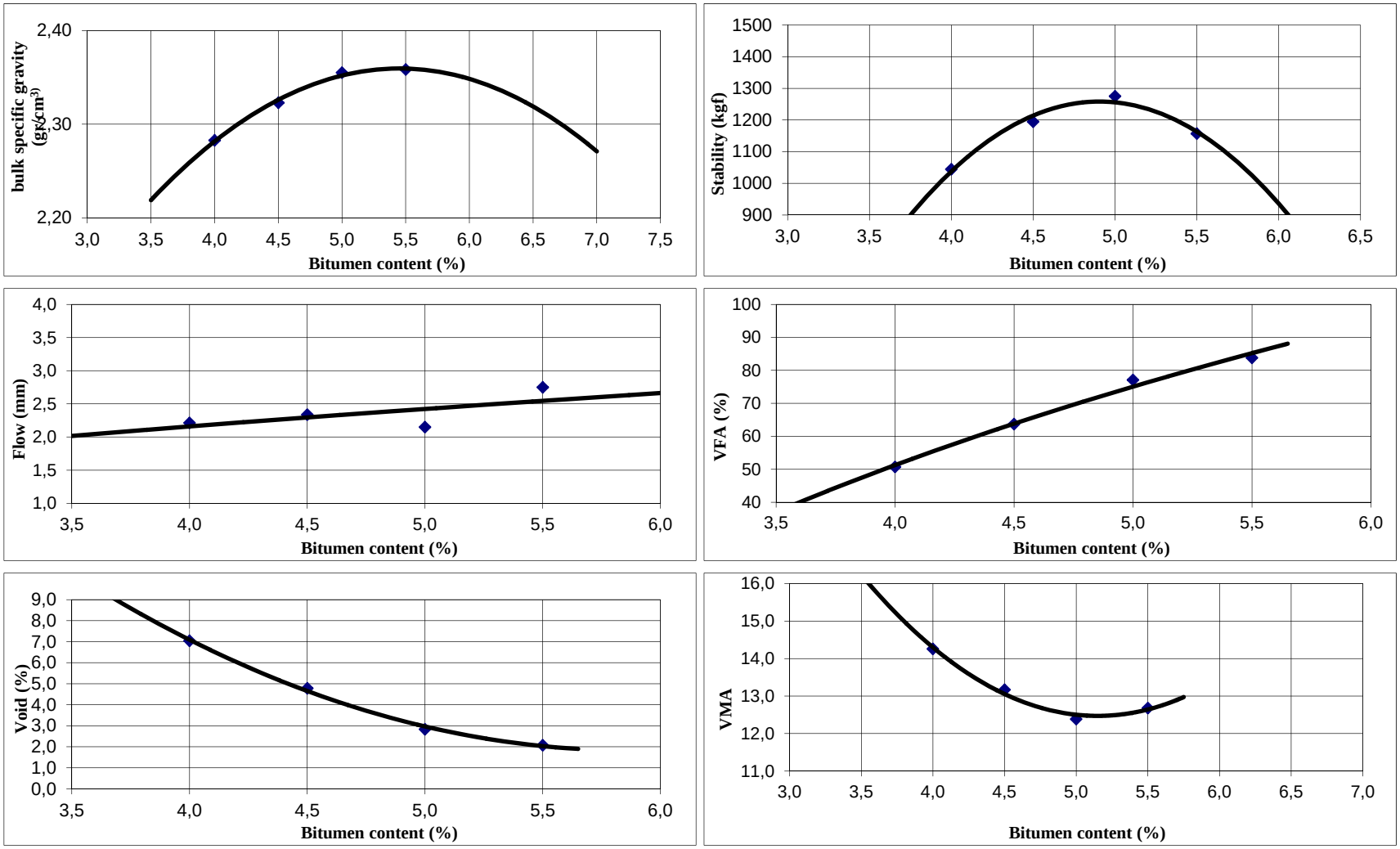

Figure A-7 Marshall mix design graphics for MJP sample

Table A-8 Marshall mix design for MRP sample

Specimen No.	Bitumen %		Specimen Height (mm)				Weight in air (gr.)	Weight in water (gr.)	SSD weight (gr.)	Volume	Bulk specific gravity	Max. teo. specific gravity	Voids (%)	VMA	VFA	Flow (mm)	Stability (kgf)	Correlation fact.	Corr. Stability (kgf)
	Wa	Wb	1	2	3	Avg.	A	C	B	V	Dp	Dt	Vh	%	%	mm	kgf		kgf
1	4.0	3.8	65.44	65.32	65.18	65.3	1171.2	662.4	1189.9	527.5	2.220	2.4386	8.953	16.61	46.1	1.95	1035	0.956	989
2	4.0	3.8	64.46	64.24	64.52	64.4	1166.5	662.1	1183.1	521.0	2.239	2.4386	8.19	15.90	48.5	2.60	1193	0.978	1167
3	4.0	3.8	65.12	65.62	65.08	65.3	1185.3	673.2	1199.7	526.5	2.251	2.4386	7.682	15.44	50.2	2.26	1301	0.956	1244
Avg.											2.237		8.274	15.98	48.3	2.27			1133
1	4.5	4.3	64.22	63.92	64.14	64.1	1184.1	676.6	1191.2	514.6	2.301	2.4227	5.025	13.99	64.1	2.02	1161	0.985	1144
2	4.5	4.3	64.26	64.50	64.18	64.3	1186.9	678.1	1196.5	518.4	2.290	2.4227	5.498	14.42	61.9	2.08	1187	0.980	1163
3	4.5	4.3	63.52	63.74	63.78	63.7	1173.5	672.5	1182.2	509.7	2.302	2.4227	4.970	13.94	64.3	2.48	1231	0.978	1204
Avg.											2.298		5.164	14.11	63.4	2.19			1170
1	5.0	4.8	64.06	64.00	64.18	64.1	1207.7	698.5	1211.8	513.3	2.353	2.4072	2.260	12.47	81.9	2.53	1182	0.995	1176
2	5.0	4.8	63.80	63.52	63.38	63.6	1177.1	677.5	1182.1	504.6	2.333	2.4072	3.094	13.22	76.6	2.54	1220	0.998	1218
3	5.0	4.8	64.12	63.90	64.26	64.1	1196.2	689.1	1198.1	509.0	2.350	2.4072	2.373	12.57	81.1	2.37	1155	1.01	1167
Avg.											2.345		2.576	12.75	79.9	2.48			1187
1	5.5	5.2	64.54	64.62	64.42	64.5	1192.6	688.6	1197.9	509.3	2.342	2.3920	2.107	13.30	84.2	2.14	1093	0.985	1077
2	5.5	5.2	64.56	64.38	64.40	64.4	1194.2	687.2	1199.8	512.6	2.330	2.3920	2.606	13.74	81.0	2.65	1036	0.978	1013
3	5.5	5.2	64.68	64.12	64.92	64.6	1188.3	682.6	1195.1	512.5	2.319	2.3920	3.069	14.15	78.3	3.46	1069	0.973	1040
Avg.											2.330		2.594	13.73	81.2	2.75			1043

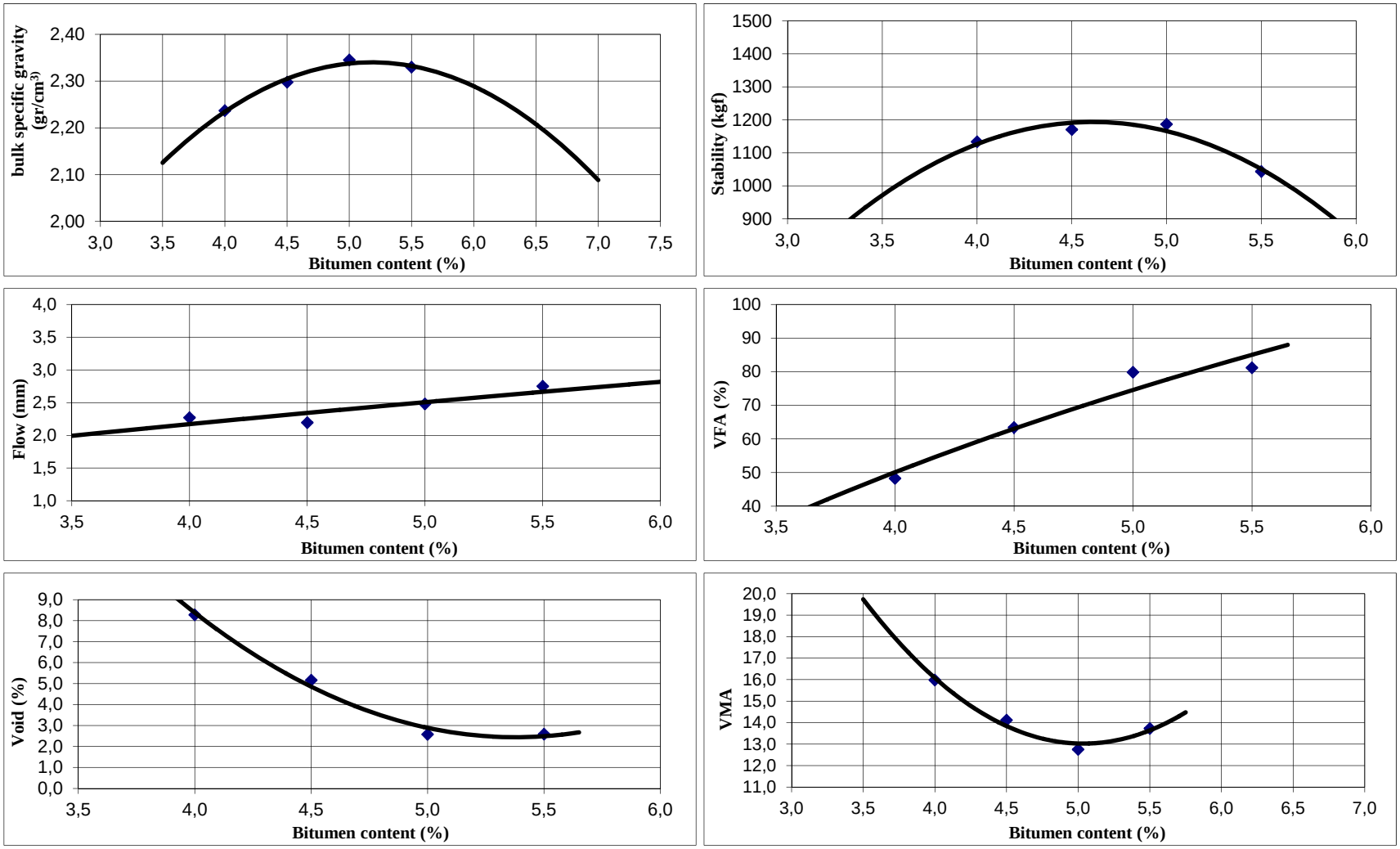

Figure A-8 Marshall mix design graphics for MRP sample

APPENDIX B

LIST OF TABLES

List of Tables

APPENDIX C

LIST OF FIGURES

List of Figures